

GRAVITY ANALYSIS OF THE SUBSURFACE  
STRUCTURE OF THE UPPER SANTA CRUZ VALLEY,  
SANTA CRUZ COUNTY, ARIZONA

by

Robert Wade Parker

---

A Thesis Submitted to the Faculty of the  
DEPARTMENT OF GEOSCIENCES  
In Partial Fulfillment of the Requirements  
For the Degree of  
MASTER OF SCIENCE  
In the Graduate College  
THE UNIVERSITY OF ARIZONA

1 9 7 8

STATEMENT BY AUTHOR

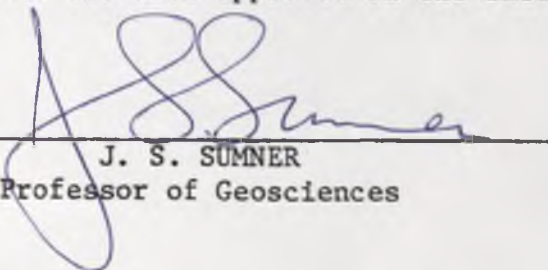
This thesis has been submitted in partial fulfillment of requirements for an advanced degree at The University of Arizona and is deposited in the University Library to be made available to borrowers under rules of the Library.

Brief quotations from this thesis are allowable without special permission, provided that accurate acknowledgment of source is made. Requests for permission for extended quotation from or reproduction of this manuscript in whole or in part may be granted by the head of the major department or the Dean of the Graduate College when in his judgment the proposed use of the material is in the interests of scholarship. In all other instances, however, permission must be obtained from the author.

SIGNED: Robert W Parker

APPROVAL BY THESIS DIRECTOR

This thesis has been approved on the date shown below:

  
\_\_\_\_\_  
J. S. SUMNER  
Professor of Geosciences

Oct 27, 1978  
Date

## ACKNOWLEDGMENTS

The work upon which this thesis is based was supported by funds provided by the U. S. Department of the Interior, Office of Water Resources and Technology Agreement Numbers 14-34-0001-7005 and -7006 as authorized by the Water Resources Research Act of 1964.

Special thanks go to GAC Properties Incorporated of Arizona and Cella, Barr, Evans and Associates of Tucson for providing topographic maps of the Rio Rico properties.

I would like to thank Dr. J. S. Sumner for his encouragement and direction throughout this project and Drs. Robert Butler and Marc Sbar for their helpful criticism during the writing of the text.

Mr. Stan Keith, of the Bureau of Geology and Mineral Technology, related some very interesting and useful observations about the structure of the study area.

Bruce Hargan's assistance and advice was invaluable in reducing the data efficiently. Another fellow graduate student, Fritz Christie, was a frequent "discussion" partner and an excellent testing ground for ideas.

A big thank you goes to everyone who provided assistance during this two year project.

## TABLE OF CONTENTS

	Page
LIST OF ILLUSTRATIONS . . . . .	vi
LIST OF TABLES . . . . .	vii
ABSTRACT . . . . .	viii
INTRODUCTION . . . . .	1
Purpose and Scope . . . . .	1
Description of Area . . . . .	3
Previous Work . . . . .	3
GEOLOGY . . . . .	6
Mountains . . . . .	6
Nogales Formation . . . . .	10
General Geologic History . . . . .	11
DATA ACQUISITION AND REDUCTION . . . . .	13
Instrumentation . . . . .	13
Field Procedures . . . . .	14
Base Station Establishment . . . . .	14
Use of Barometer . . . . .	15
Field Station Selection Requirements . . . . .	15
Gravity Anomalies . . . . .	16
Gravity Data Reduction . . . . .	18
Time Variations . . . . .	19
Position Corrections . . . . .	20
Error Analysis . . . . .	21
Density Data . . . . .	23
INTERPRETATION . . . . .	26
Free-air Gravity Anomaly Map . . . . .	26
Complete Bouguer Anomaly Map . . . . .	27
Regional-residual Calculation and Separation . . . . .	28
Regional Elevation Datum . . . . .	28
First Order Residual Bouguer Anomaly Map . . . . .	29
Bedrock Surface . . . . .	31
Second Order Residual Map . . . . .	32
Two Dimensional Modeling . . . . .	32
Density Contrast . . . . .	35

TABLE OF CONTENTS--Continued

	Page
Profile Analysis . . . . .	36
Depth to Bedrock and Basin Structure Map . . . . .	45
Ground Water Available from Storage . . . . .	45
Errors in Interpretation . . . . .	48
Correlation with Aeromagnetic Data . . . . .	51
CONCLUSIONS . . . . .	53
REFERENCES . . . . .	55

## LIST OF ILLUSTRATIONS

Figure	Page
1. Arizona Gravity Thesis Research Areas . . . . .	2
2. Sketch Map of Upper Santa Cruz Valley and Vicinity . .	4
3. Geologic Map . . . . .	In pocket
4. Free-air Gravity Anomaly Map . . . . .	In pocket
5. Complete Bouguer Anomaly Map . . . . .	In pocket
6. First Order Regional Anomaly Map: Regional Elevation Datum . . . . .	30
7. First Order Residual Bouguer Anomaly Map: Regional Elevation Datum . . . . .	In pocket
8. Regional Bedrock Surface Map . . . . .	33
9. Second Order Residual Bouguer Anomaly Map: Bedrock Surface Removed . . . . .	In pocket
10. Profile A-A' . . . . .	37
11. Profile B-B' . . . . .	38
12. Profile C-C' . . . . .	39
13. Profile D-D' . . . . .	40
14. Profile E-E' . . . . .	41
15. Profile F-F' . . . . .	42
16. Subsurface Basin Configuration: Interpretation Map . .	In pocket
17. Residual Aeromagnetic Map of the Upper Santa Cruz Valley (from Sauck and Sumner, 1970) . . . . .	52

LIST OF TABLES

Table	Page
1. Density Data . . . . .	24
2. Average Rock Densities . . . . .	25
3. Volume of Saturated Alluvium . . . . .	47
4. Volume of Ground Water Available . . . . .	49

## ABSTRACT

A gravity survey was conducted in the Upper Santa Cruz Valley, Santa Cruz County, Arizona. Residual gravity anomalies were interpreted to define the subsurface structure and to estimate the water resource potential.

A north-south trending fault system with at least 2000 ft of vertical displacement forms the western half of the basin graben structure. The eastern basin boundary is a combination of northwest- and northeast-trending scarps. These scarps are all extensions of or parallel to inferred surface faultly traces. The valley is divided into three major sections, each having a maximum thickness of 4200 ft of alluvium. Alluvium-covered pediments are present on both sides of the valley.

The total volume of ground water available in storage in the Upper Santa Cruz Valley is calculated to be 24.3 million acre feet. This total volume of water is not entirely recoverable, because of permeability factors.

The alluvium-covered area east of Nogales is not a basin, but rather is a pediment surface. An alluvium-covered area near Ruby is not sufficiently deep to be a major water resource. A two mile wide gravity low just northwest of Nogales contains about 2200 ft of alluvium and is the dominant subsurface feature of the southern third of the valley.



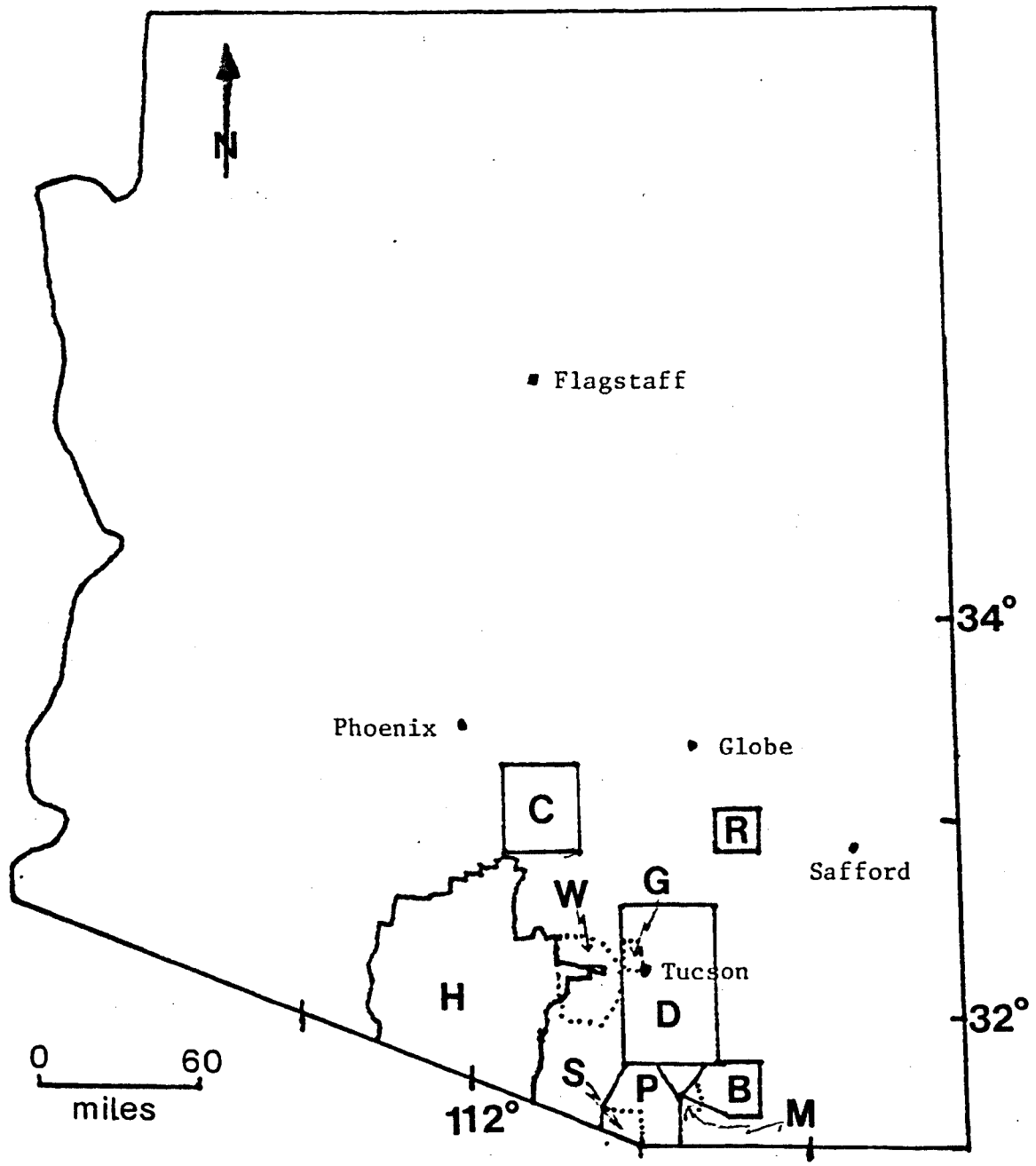
## INTRODUCTION

One of the most pressing problems facing Arizona's Sonoran Desert region is the availability, distribution, and allocation of subsurface water resources. The Tucson area is especially dependent on ground water and the farms, mines, and people are all competing for the same water.

Determination of the subsurface basement configuration in individual valleys using gravity techniques is one method of estimating the availability and distribution of ground water, as well as defining pediment surfaces for mineral exploration. Gravity surveys have been completed by Hargan (1978) in the Papago Indian Reservation, Bittson (1976) in the Cienega Creek area, Robinson (1975) in the Aravaipa Valley, and Goodoff (1975) in the Cortaro Basin (Figure 1). Additional calculations to determine the volume of ground water available from storage in the basin have been performed by West (1970a) in Avra Valley and Davis (1967) in the Tucson Basin.

### Purpose and Scope

This thesis reports a detailed gravity survey of the Upper Santa Cruz Valley in Santa Cruz County. Determination of the subsurface basement configuration and the ground water storage potential were the primary goals. These were achieved through the compilation and interpretation of residual gravity anomaly maps and two dimensional profiles.



- |                                    |                                  |
|------------------------------------|----------------------------------|
| <b>P</b> This study                | <b>B</b> Bittson (1976)          |
| <b>C</b> Christie (in preparation) | <b>D</b> Davis (1967)            |
| <b>G</b> Goodoff (1975)            | <b>M</b> Menges (in preparation) |
| <b>H</b> Hargan (1978)             | <b>R</b> Robinson (1975)         |
| <b>S</b> Hench (1968)              | <b>W</b> West (1970a)            |

Figure 1. Arizona Gravity Thesis Research Areas.

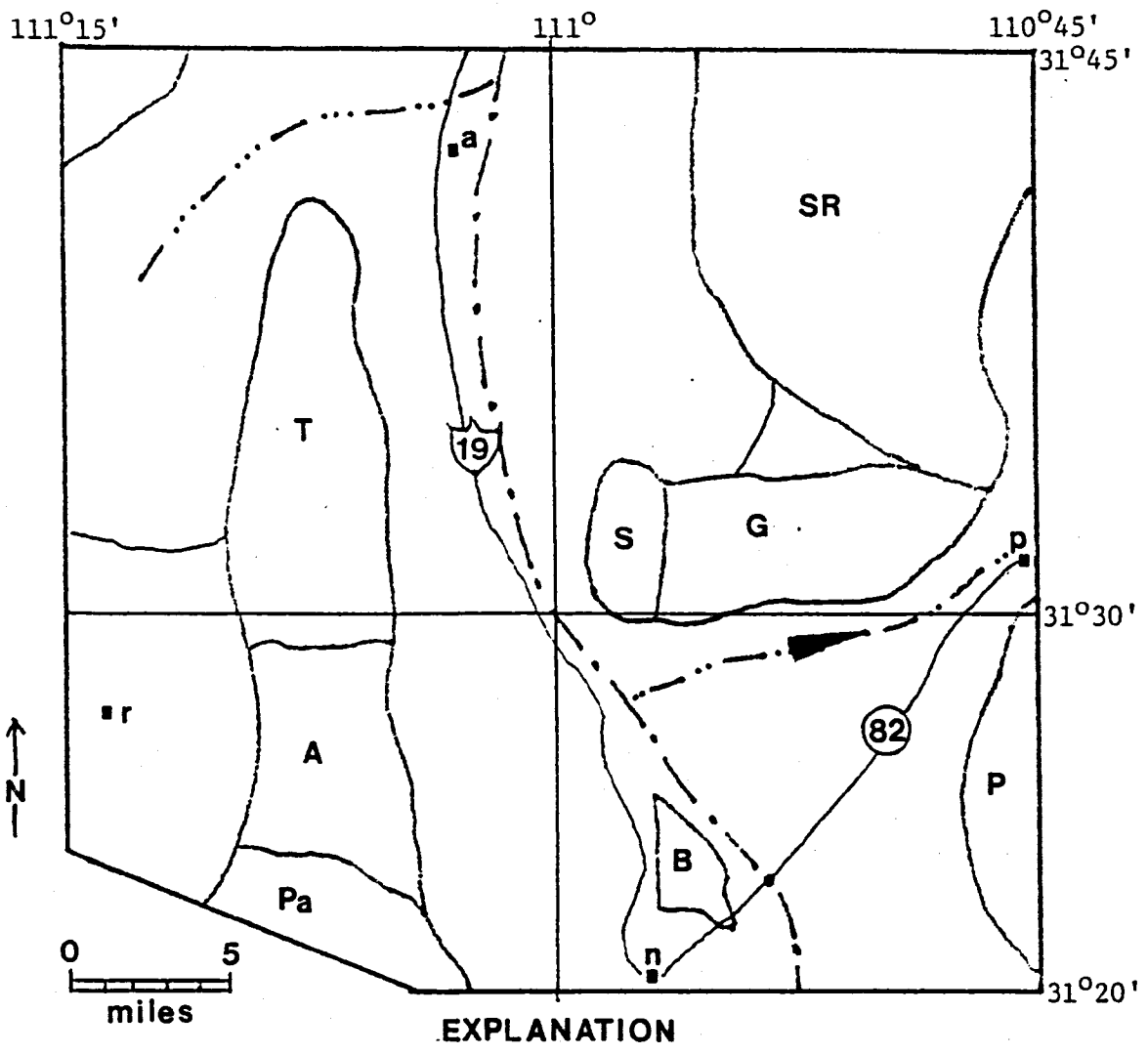
### Description of Area

The Santa Cruz Valley trends in a northerly direction from Nogales to Tucson. Only the portion of the valley in Santa Cruz County, beginning 35 miles south of Tucson, will be discussed (Figure 2). Bounding the thesis area to the north and south are two political boundaries, those of Santa Cruz County and Mexico, respectively. The eastern boundary of the primary study area is formed by the Santa Rita Mountains, Grosvenor Hills, San Cayetano Mountains, and intrusives in the Nogales area. To the west are the rugged Pajarito, Atascosa, and Tumacacori Mountains.

The Santa Cruz River enters the primary valley from the southeast approximately 8 miles north of Nogales. A secondary study area includes the course of the river east of Nogales and is bounded to the north by the Grosvenor Hills and east by the Patagonia Mountains. Alluvial fill in the Ruby area west of the primary valley is also included as a secondary study area.

### Previous Work

Several geologists have worked in the mountains of Santa Cruz County. Drewes (1971, 1972) has done extensive work in the Santa Rita Mountains and has mapped the Mt. Wrightson 15 minute U.S. Geological Survey Quadrangle. Simons (1974) has mapped the Nogales Quadrangle. Cunningham (1964) studied extensively a small area of the North Tumacacori Foothills, and Nelson (1963) worked in the southern Atascosa and Pajarito Mountains. Webb and Coryell (1954) did some preliminary regional mapping in the Ruby Quadrangle. Wilson, Moore, and Cooper (1969)



**EXPLANATION**

- |                                 |                                |
|---------------------------------|--------------------------------|
| <b>T</b> Tumacacori Mountains   | <b>a</b> Amado                 |
| <b>A</b> Atascosa Mountains     | <b>r</b> Ruby                  |
| <b>Pa</b> Pajarito Mountains    | <b>n</b> Nogales               |
| <b>P</b> Patagonia Mountains    | <b>p</b> Patagonia             |
| <b>B</b> Mount Benedict area    | <b>- - -</b> Santa Cruz River  |
| <b>S</b> San Cayetano Mountains | <b>- · - · -</b> Sonoita Creek |
| <b>SR</b> Santa Rita Mountains  | <b>· · · - -</b> Sopori Wash   |
| <b>G</b> Grosvenor Hills        |                                |

Figure 2. Sketch Map of Upper Santa Cruz Valley and Vicinity.

present the general geology of the entire area in their "Geologic Map of Arizona".

Hench (1968) did a detailed gravity survey of the Ruby quadrangle, concentrating on a collapse caldera in the Pena Blanca Lake area. Plouff (1961) did a gravity survey for the U. S. Geological Survey of the Tucson area which extended into the northernmost portion of this study area. Davis' (1967) dissertation on the Tucson Basin also extends about 3 miles into the northern section of the study area. Additional gravity stations on a regional basis have been established over the years for The University of Arizona's Laboratory of Geophysics Gravity Data Base. State maps using all available data have been published by West and Sumner (1973); Aiken, Schmidt, and Sumner (1975); and Aiken (1975). Aeromagnetic data of the area have been compiled and published by Sauck and Sumner (1970). Bradbeer (1978) conducted a hydrogeologic evaluation of the Sonoita Creek aquifer.

## GEOLOGY

The Upper Santa Cruz Valley is typical of southern Arizona's Basin and Range Province. It is dominated by north-northwest trends in mountain ranges and basins resulting from Miocene block faulting during the Basin and Range Orogeny. Also common in the Basin and Range Province is a very complicated geologic history due to several previous periods of tectonic activity. The mountainous regions of the study area are as complex as any in Arizona.

### Mountains

The Santa Rita Mountains are the most prominent feature of the study area, reaching an elevation of 9453 ft (2881 m). The rocks of the Santa Rita Mountains are abundantly faulted and less commonly folded. Drewes (1972) defines three major structural units, all bounded by major fault zones. Only the Southwestern Structural Unit (Drewes, 1972), which underlies the southwest flank of the Santa Rita Mountains as well as the Grosvenor Hills and San Cayetano Mountains, is in the study area.

The northeast boundary of the Southwestern unit is the pre-Mesozoic Santa Rita Fault Scar, a fault zone largely obscured by Mesozoic plutons (Drewes, 1972). These plutons appear in Figure 3 (in pocket) as Kqm and Jg. Outside the primary study area northeast of the Santa Rita Fault Scar is a thick sequence of Mesozoic latitic and rhyolitic volcanics and andesite flows.

Drewes (1972) divided the Southwestern Structural Unit into four blocks, each bounded by faults. The southwesternmost of these is the San Cayetano block, which includes the San Cayetano Mountains and pediments and is separated from the Grosvenor Hills block by the north-trending San Cayetano fault. The southern two-thirds of the San Cayetano block are underlain by a gently southward dipping sequence of volcanic and sedimentary rocks of the upper members of the late Late Cretaceous Salero Formation (Drewes, 1972). These are intruded by latest Late Cretaceous Josephine Canyon diorite and Oligocene quartz latite porphyry dikes. The northern third is primarily Tertiary volcanic and sedimentary rocks which dip very gently eastward or westward (Drewes, 1972).

The Grosvenor Hills block lies between the San Cayetano fault and Salero fault zone (Figure 3). The dominant geologic feature is the Grosvenor Hills volcanics, consisting of a basal gravel and silt member, a tuff-rich rhyolite member, and a capping rhyodacite member, all of late(?) Oligocene age (Drewes, 1972). To the east and north, the underlying Upper Cretaceous rocks extend from beneath the volcanic field and overlie Jurassic and Precambrian rocks (Drewes, 1972). The volcanics outcrop in a downdropped area between the two bounding faults and most faulting in the Grosvenor Hills is high-angle and restricted to the volcanic field.

The Salero fault zone trends northwesterly from near Patagonia in the southeast into the pediment area west of the Glove Mine near Cottonwood Canyon. Several episodes of displacement can be identified

with total movement many thousands of feet up to the northeast (Drewes, 1972).

The Montosa Canyon block is a small structural block north of the Salero and Grosvenor Hills blocks and south of the Miocene range front Elephant Head fault. Besides Precambrian rock, the entire Paleozoic sequence and even Mesozoic rock can be identified here. Abundant thrust faults and normal faults complicate the geology (Drewes, 1972).

The northeasternmost and least disturbed block is the Salero. It is bounded generally by the Elephant Head and Salero faults and the Santa Rita Fault Scar. The block is underlain by granitoid Jurassic and Cretaceous rocks. Several swarms of dikes and quartz veins intrude these rocks.

The Patagonia Mountains are southeast of the Santa Rita Mountains. Many of the intrusives and volcanics are common to both ranges (Drewes, 1972; Simons, 1974). Basic structural similarities can be seen in the general northwest trend of major faults, granitic rocks west of a Mesozoic Volcanic sequence, and a northeast-trending range front fault which forms the northern boundary.

Only the western third of the Patagonia Mountains is in the study area. Outcrops of Jurassic Comoro Canyon Granite (Jg on Figure 3) and Precambrian quartz monzonite and hornblende-rich granodiorite (pC on Figure 3) extend from the western flank of the mountains up to 4 miles from the pediment area. A large body of Paleocene biotite hornblende granodiorite (Tg on Figure 3) is present east of the Precambrian rocks. Massive sulfide ore bodies are found throughout the Patagonia Mountains.



East of the Patagonia Mountains and 5 miles north of Nogales is a small (10 square miles) mountainous area of Jurassic Mount Benedict Quartz Monzonite (Jg on Figure 3). These mountains were uplifted by young (less than 12 m.y.) normal faulting (Simons, 1974).

The Pajarito, Atascosa, and Tumacacori Mountains form the western border of the study area. No comprehensive field work has been attempted here and knowledge is therefore sketchy. A large area of the Tumacacori Mountains is overlain by an ignimbrite field (S. Keith, personal communication, 1978). Early Tertiary-Late Cretaceous granitic rocks and metamorphosed Permian(?) limestones are identified north of the ignimbrite. Cretaceous andesitic flows and tuffs (Ka on Figure 3) contact the ignimbrite field in several locations in all directions and may also underlie the ignimbrite field.

Nelson (1963) has described the rocks of the Pajarito and Atascosa Mountains. He considers the Cretaceous andesite (Ka on Figure 3) and Laramide Granite (TKg on Figure 3) of the southeast Pajarito Mountains to be contemporaneous and calls them the Pajarito Lavas. Directly to the west, Cretaceous sediments overlie the Pajarito Lavas and comprise the Oro Blanco Conglomerate (Kb on Figure 3). To the north a younger Cretaceous andesite (Ka on Figure 3) forms the Montana Peak Formation and overlies the Oro Blanco Conglomerate (Nelson, 1963). Tertiary rhyolites unconformably overlie the Montana Peak Formation and are assumed to be associated with the volcanics (Tvs on Figure 3) of the Tumacacori Mountains. Motion on the two north-south trending faults seen on Figure 3 caused the uplift of the Atascosa Mountains (Webb and Coryell, 1954).

### Nogales Formation

The Nogales Formation is of special importance in this study because it is intermediate in density (see "Interpretation"), and was faulted during Basin and Range tectonic activity. It is not considered as bedrock in this study (see "Interpretation"). Exposures of Nogales Formation (Tn in Figure 3) are near Cottonwood Canyon in the Mt. Wrightson Quadrangle, in several localities near Nogales, and possibly just east of the Atascosa Mountains in the Ruby Quadrangle. Simons (1974, p. 5) has defined the Nogales Formation as follows:

The Nogales Formation is here named for exposures in, east, and north of the town of Nogales which are designated the type area. Rocks believed to be correlative with the Nogales Formation are exposed also along and south of Sonoita Creek. The total outcrop area of the formation within the Nogales quadrangle is 35 to 40 square miles. The Nogales Formation rests on, and in part is derived from, Grosvenor Hills Volcanics of Oligocene age; it is overlain by poorly consolidated alluvium believed to be of late Tertiary and Quaternary age. Its most likely age, therefore, is late Tertiary.

Rocks that on the basis of lithology and stratigraphy are probably of about the same age as the Nogales Formation crop out in the Ruby quadrangle 5 to 6 miles west of Calabasas. The groundmass of a basalt flow intercalated in these rocks has been dated by the potassium-argon method at  $12.6 \pm 0.8$  m.y. (R. F. Marvin, H. H. Mehnert, and V. M. Merritt, written communication, 1970).

Simons (1974) divided the Nogales Formation into three members. The upper member consists of as much as 2000 ft of epiclastic volcanic conglomerate. The middle member is a bedded pebbly to bouldery tuffaceous sandstone and subordinate tuff about 500 ft thick. The lower member of light gray to light brown conglomerate, fanglomerate, tuffaceous conglomerate and sandstone, and tuff may be 5000 ft thick. Some thin basalt flows and dikes are also present (Simons, 1974).

### General Geologic History

The following discussion draws heavily from conclusions by Simons (1974). Application of his conclusions to the Tumacacori, Atascosa, and Pajarito Mountains are interpretations of the author.

The oldest rocks in the study area are the Precambrian (800-1600 m.y.) igneous rocks of the west flank of the Patagonia and Santa Rita Mountains. Uplift and erosion of these rocks was followed by non-continuous deposition in a near-shore environment of about 4600 feet of Paleozoic rocks.

Uplift, faulting, and differential erosion in late Paleozoic to early Mesozoic time left an area of high relief. Continued faulting and erosion was accompanied by deposition of at least 7000 feet of Triassic and Jurassic silicic volcanics in the eastern Santa Rita and Patagonia Mountains. Emplacement of granitic plutons in the Precambrian rocks west of the Patagonia Mountains during middle Jurassic time was correlated with similar activity in the central Santa Rita Mountains and Mount Benedict area. Another episode of uplift and erosion during Late Jurassic and Early Cretaceous time was followed by large-scale faulting and profound erosion. This Late Cretaceous faulting was believed to be an early manifestation of the Laramide orogeny.

Widespread deposition of volcanic and subordinate sedimentary rocks occurred in late Late Cretaceous time. Outcrops of this type are seen in upper Sonoita Creek, southern San Cayetano Mountains, southern Atascosa and Pajarito Mountains, and along the Santa Cruz River east of Nogales. Emplacement of the monzonite and granodiorite along the Santa Rita fault scar occurred in latest Late Cretaceous (Drewes, 1972).

The large body of biotite hornblende granodiorite in the southern Patagonia Mountains was intruded in early Tertiary time. Widespread alteration and mineralization associated with the emplacement seemed to end by mid-Tertiary time.

Deposition of several thousand feet of rhyodacitic and rhyolitic lava and tuffs formed the Oligocene Grosvenor Hills Volcanics. This is possibly contemporaneous with the large ignimbrite field in the Tuma-cacori Mountains. Uplift in the region was accompanied and followed by long continued deposition of up to 7500 feet of Nogales Formation.

Basin and Range faulting (12-5 m.y. ago) began and is illustrated by faulting of Nogales Formation during uplift of the Mount Benedict and San Cayetano Mountain areas. Minor fault movement still occurs today, as scarps can be seen in alluvium along the Elephant Head Fault north of the Santa Rita Mountains.

The last few million years are characterized by major erosion and widespread alluviation. These unconsolidated and partially consolidated deposits are the primary source of water in the Basin and Range Province.

## DATA ACQUISITION AND REDUCTION

Data for this study were collected from September, 1976 to January, 1978. A total of 336 new gravity stations were added to The University of Arizona Laboratory of Geophysics Gravity Data Base. A gravity station is defined as the location where data are taken. Information recorded at each station includes time and date, location, at least three readings of the meter (only the weighted average is used for observed gravity), accuracy, general geology, elevation and elevation control, and sometimes directions to the station, and terrain in the area of the station.

### Instrumentation

Gravity measurements were made using LaCoste & Romberg astatic gravimeters. All but nine stations were acquired with The University of Arizona's meter, Model G, number 174. Arizona State University's Meter G359 was used for one day.

LaCoste & Romberg geodetic model gravimeters measure relative changes in the vertical component of the earth's gravitational field. Changes in gravity are registered by changes in length of a spring, whose length is assumed to be zero when no forces are acting upon it. This highly mobile instrument is kept at constant temperature to control thermal expansion and has an accuracy of one part in  $10^8$  (.01 mgal). The drift rate is less than 1 mgal per month (LaCoste and Romberg, 1968). More detailed discussions of the operation of gravimeters may

be found in Dobrin (1960) and Nettleton (1976), and a discussion of Model G may be found in West (1970a).

### Field Procedures

#### Base Station Establishment

Three base stations were used for drift control in this study. All three are established relative to the Potsdam (in 1930) datum. The main base station was The University of Arizona Geology Building (observed gravity = 979253.841 mgal). An established base station at Nogales International Airport (observed gravity = 979068.941 mgal) was used as a secondary field base. A primary field base station was established for this study at a bench mark in the school yard at Arivaca Junction, one mile west of I-19, 250 yards north of Arivaca Road. This station was read a total of 28 times before being inserted into the base station network. Five of these readings were not included in the determination because of high winds or disturbances due to children and sprinklers. These conditions were avoided after the station was established. Reductions were made relative to the Geology Building base, and the observed gravity at Arivaca Junction was computed to be 979144.034 mgal. A standard deviation of .079 mgal was calculated for the 23 readings used while the standard deviation of all 28 readings was .080 mgal. (Further discussion of these values is included in "Error Analysis".)

## Use of Barometer

One gravity loop was conducted with the aid of a barometer. Usually elevations from barometers are questionable, but special conditions made the accuracy of the stations  $\pm 3$  ft or better.

The loop was conducted along Mt. Hopkins Road in Amado from a bench mark at the railroad uphill to a surveyed elevation at an intersection five miles east. Station locations were predetermined and elevation increased at each station from the railroad to the intersection.

The survey was run early in the morning (6:00 a.m.) to limit changes in barometric pressure, and each station was occupied three times. In all cases, agreement in elevation was within two feet. A second barometer left at the railroad bench mark recorded no pressure changes. Relative humidity and temperature were also monitored.

It was found that an error of 14 feet in elevation was recorded between the two control points. This was removed in the same manner as drift in a gravimeter because elevations of stations along the loop steadily increased. A final check of elevations by interpolating contours on U. S. Geological Survey topographic maps of the area was very favorable.

## Field Station Selection Requirements

A station interval of one per square mile was acquired where data and roads were accessible. A total of 39 days were spent gathering 336 field stations. Bench marks accurate to  $\pm .1$  ft or better comprised almost 31% of the stations and surveyed elevations and photo control

points accurate to  $\pm 1$  ft accounted for 207 stations. Hence, 92.2% of all new stations were accurate to  $\pm 1$  ft. The remaining 26 stations were accurate to  $\pm 5$  ft in elevation or less. Latitudes and longitudes were chosen to the nearest .01 minute.

Two hundred forty-four additional stations were chosen from the Arizona Gravity Data Base. All but 16 of these are in the Ruby 15 minute quadrangle. The stations in the Ruby quadrangle do not satisfy the elevation and position requirements, but there is little elevation control in the area due to rugged topography and no roads. All of the Ruby data is from Hench (1968). (See additional discussion under "Error Analysis".)

#### Gravity Anomalies

The gravity anomalies of interest in this study are those caused by near-surface density inhomogeneities; that is, differences in density between bedrock and alluvium. Dobrin (1960, p. 190) defines a gravity anomaly as "the departure of a corrected gravity value from the theoretical value of gravity on the spheroid at the latitude and longitude of the station." Nettleton (1954) includes regional anomalies (those not of interest to an investigator) and residual anomalies (those that reflect sources of interest) in a study in his definition.

Two anomalies are usually calculated for gravity surveys. These are the free-air and complete Bouguer anomalies. Maps of each anomaly will be discussed under separate headings.



The free-air anomaly is due to variations in gravity with elevation above sea level. This value is easily calculated by differentiation after manipulations of Newton's law of gravitation. That is (Garland, 1976):

$$F = G \frac{M_e m}{R^2}; \text{ Newton's Law of Gravity} \quad (1)$$

$$\text{and } g = F/m \text{ from Newton's second law of motion} \quad (2)$$

$$\text{thus } g = \frac{GM_e}{R} \quad (3)$$

And to a first approximation

$$\frac{\partial g}{\partial R} = \frac{-2GM_e}{R^3} = \frac{-2g}{R} \quad (4)$$

where  $G$  = gravitational constant

$M_e$  = mass of Earth

$m$  = any mass

$R$  = radius of Earth

$g$  = gravitational acceleration.

Equation (4) is the vertical gradient of gravity; the value of which,  $-0.09406$  mgal/ft, is the free-air correction (Garland, 1970).

The free-air gravity anomaly is equal to

Observed grav - Free-air correction - Theoretical gravity.

The formula for theoretical gravity used in this study is the 1930 International Gravity Formula:

$$\delta_o = 978049 (1 + 0.0052884 \sin^2\phi - 0.0000059 \sin^2 2\phi) \quad (5)$$

where  $\delta_o$  = theoretical gravity

$\phi$  = latitude of station.

Excess mass above sea level not accounted for with the free-air correction is removed by the Bouguer slab correction. The assumption is that the excess mass between sea level and the station be treated as an infinite horizontal slab of thickness equal to the elevation of the station. A derivation of the formula may be found in Garland (1970). The attraction of such a slab,  $\Delta g$ , is dependent on density,  $\rho$ , and elevation,  $h$ , and is equal to

$$\Delta g = 2\pi G\rho h \quad (6)$$

A density of  $2.67 \text{ g/cm}^3$  was used in this study. This density has been shown by Sumner and Schnepfe (1966) to be applicable in southern Arizona and it has been used successfully in every thesis shown in Figure 1. The Bouguer correction is  $-0.03408 \text{ mgal/ft}$  when  $\rho = 2.67$ . The Bouguer gravity anomaly is equal to

Observed gravity + Free-air correction - Bouguer  
correction + Topographic correction - Theoretical  
gravity

Regional anomalies are usually removed from the complete Bouguer anomaly for interpretation of the residual anomaly.

#### Gravity Data Reduction

Reduction of gravity data to the complete Bouguer anomaly was accomplished through the use of the Fortran XGRAV program by West (1970b)

and updated by James Schmidt, University of Arizona, Department of Geosciences, and a terrain correction program, TERAN, written by Plouff (1966) and adapted to the University's computer systems by James Schmidt.

#### Time Variations

After the dial reading has been converted to milligals using tables unique to each meter, the effect of Earth tides must be calculated. The tidal effect of the sun and moon can vary as much as .3 mgal during the course of a day (Hammer, 1939; Dobrin, 1960, p. 234). A subroutine in the XGRAV program calculates this effect. Nettleton (1976, p. 76) gives an equation for the tidal gravitational effects as

$$g = \frac{3GrM_m}{2D_m^3} \left( \cos 2\alpha_m + \frac{1}{3} \right) + \frac{3GrM_s}{2D_s^3} \left( \cos 2\alpha_s + \frac{1}{3} \right) \quad (7)$$

where  $r$  = radius of Earth

$M$  = mass

$D$  = distance from Earth

$\alpha$  = geocentric angle

$m$  = moon

$s$  = sun

Instrument drift also affects the observed gravity at a station. These variations are assumed to be linear and are removed by comparing base station values after external time variations are removed. The average drift of meter G174 was 0.0065 mgal/hr with an RMS deviation of 0.0247 mgal. All observed station loops were 13 hours or less in duration. Drift rates are directly affected by reader error; high drift

rates (greater than  $\pm 0.04$  mgal/hr) are believed by the author to be the result of reader error and not instrument drift (see additional discussion in Error Analysis section).

#### Position Corrections

Corrections are applied to each station which are unique to that station. These are calculated after tide and drift corrections and are functions of elevation, latitude, or terrain. The free-air and Bouguer slab corrections are functions of elevation and have been described in the section on "Gravity Anomalies."

Acceleration of gravity varies by +5000 mgal from the equator to the poles. At  $45^{\circ}$  latitude, this change is about 0.1 mgal for each 400 ft of displacement in the north-south direction (Dobrin, 1960, p. 234). This effect is removed by the International Gravity Formula for theoretical gravity (eq. 5).

Because the Bouguer correction assumes an infinite horizontal slab for the earth, a curvature correction must be applied. This correction has been incorporated into the terrain correction program and varies with elevation,  $h$  (ft), above sea level. The curvature correction (CC) used in TERAN (Plouff, 1966) is:

$$CC = 1.2 \times 10^{-15}h^3 - 3.282 \times 10^{-8}h^2 + 4.462 \times 10^{-4}h \quad (8)$$

Terrain corrections were calculated using 1 minute blocks digitized from topographic maps for the 2.5-21.0 km distance from the station. Three minute blocks were used for calculations from 21-60 km from the station. Hammer charts were used for inner hand corrections

(Dobrin, 1960, p. 232-233) from 150 m to 2.5 km. Only selected stations near bedrock were hand corrected. Terrain corrections are always added to the Bouguer anomaly values because any deviations from a uniform plane (hills and valleys) will tend to decrease the value of gravity.

#### Error Analysis

The first source of error is in the accuracy of the reading and possible non-linearity of instrument drift. Nettleton (1976, p. 35) states the observational accuracy of the LaCoste-Romberg gravimeter as being on the order of 0.01 mgal. The Laboratory of Geophysics meter G174 is not equipped with a galvanometer and it is difficult if not impossible to achieve repeatability to 0.01 mgal using this instrument. It is the author's belief that the standard deviation of base station readings (see "Base Station Establishment"), 0.079 mgal, is a more accurate estimate of reader and instrument error. LaCoste and Romberg (1968) claim a linear drift in Model G meters and there is no proof to the contrary. No separate error will be calculated for drift, because any non-linear drift would appear as reader error. Hench (1968) used a Worden Gravimeter (Educator model) in his study. The sensitivity of this meter is 0.01 mgal (Telford et al., 1976).

Hargan (1978, p. 34) shows that the variation between the tide tables and computer-calculated tide corrections is less than 0.01 mgal. West (1970a) estimated that the errors in the tide tables rarely exceed  $\pm 0.01$  mgal. A total tide error of  $\pm .02$  mgal will be used in this study.

The accuracy of  $\pm 1$  ft in elevation of 310 of the new stations gathered in this study contributes an error of  $\pm .06$  mgal to the complete Bouguer anomaly. Hensch (1968, p. 5) claims a maximum error of  $\pm 5$  ft for his data. This would cause an error of  $\pm .3$  mgal for his data and the remaining 26 new stations gathered.

All of the data are plotted on 15 minute U. S. Geological Survey topographic maps. The maximum positioning error according to National Map Accuracy Standards (Marsden, 1960) is 100 ft (31 m). This results in an error of  $\pm 0.023$  mgal in computed theoretical gravity. Hensch's (1968) data are accurate to 0.1 minute (approximately 500 ft) and a position error of 0.115 mgal results.

The greatest source of error in this study is in the terrain correction. The program TERAN produces very repeatable terrain corrections and no errors are assumed from computer corrections. Near station correction errors are difficult to estimate. A few valley stations were hand corrected and found to need less than 0.1 mgal correction. All near mountain stations were corrected and maximum corrections rarely exceeded 1 mgal. However, an error of as much as .5 mgal probably exists in a few non-corrected hilly areas and corrected mountainous stations. All of Hensch's (1968) stations are located in high relief areas.

The root mean square of independent errors (Bevington, 1969) used by Bittson (1976) and Hargan (1978) will be used in this study. The maximum error in complete Bouguer anomaly values is given by the equation

$$E_T = (E_1^2 + E_2^2 + \dots + E_n^2)^{1/2} \quad (9)$$

where  $E_T$  is the total error and  $E_n$  are the errors determined from independent calculations. The error associated with valley stations (greater than 3 km from the mountain front) is  $\pm 0.144$  mgal and for near mountain stations the error is  $\pm 0.510$  mgal. Hench's (1968) data, almost all of which is out of the primary study area, has an error of  $\pm 0.600$  mgal.

#### Density Data

Representative bedrock samples were gathered at all stations on outcrop. Dry densities were calculated using the buoyancy method. Observed densities are presented in Table 1 and must be considered minimum values. All specimens were weathered and not compacted because they were from surface outcrops.

Table 2 summarizes density samples from recent gravity theses at The University of Arizona. These data support the assumption that the average near-surface crustal density is 2.67 g/cc in southern Arizona.

Table 1. Density Data.

Rock Type	No. of Samples	Range g/cc	Mean g/cc
Nogales Formation	9	2.01-2.55	2.24
Tertiary rhyolitic tuff (Tumacacori Mountains)	5	2.28-2.50	2.38
Tertiary-Cretaceous granitic rocks (Tumacacori Mountains)	6	2.54-2.72	2.63
Altered Cretaceous andesitic rocks (2 miles west of Pena Blanca Lake)	6	2.33-2.45	2.38
Jurassic quartz monzonite (Mount Benedict)	4	2.55-2.69	2.62
Other Jurassic granitic rocks	4	2.53-2.79	2.63
Metamorphosed sedimentary rock (Naco Group?)	2	2.70-2.83	2.76
-----			
Average volcanic rocks		2.38 g/cc	
Average intrusive rocks		2.63 g/cc	
Average metamorphic rocks		2.76 g/cc	



Table 2. Average Rock Densities.

	Sedimentary Bedrock g/cc	Volcanic Rock g/cc	Intrusive and Metamorphic Rocks g/cc	Older Alluvium g/cc	Nogales Formation g/cc
From Table 1 (Dry)	--	2.38	2.66	--	2.24
Hargan (1978) (Dry)	2.71	2.48	2.62	--	--
Bittson (1976) (Wet)	2.58	2.61	2.62	--	--
Robinson (1975) (Wet)	2.55	2.42	2.58	2.07	--
West (1970a) (Wet)	2.62	2.62	2.65	--	--
Hench (1968) (Wet)	2.47	2.56	2.66	2.05	2.13 <sup>a</sup>
Davis (1967) (Wet)	2.66	2.56	2.66	--	--

<sup>a</sup>This density is the average of volcanic conglomerate, breccia, and tuff densities.

## INTERPRETATION

### Free-air Gravity Anomaly Map

The Free-air Gravity Anomaly Map (Figure 4, in pocket) has been contoured at a 5 mgal interval instead of 2 mgal, as on the accompanying gravity maps, because of the strong gradients and high amplitudes of the free-air gravity anomalies. These high-amplitude short wavelength free-air anomalies closely correlate with local variations in topography; there being more mass between the station and the center of the earth on a hill than in a valley (Aiken, in preparation). Smoothed elevation contours from 3000-4000 ft at 250 ft intervals have been included on this map to help illustrate the relationship between free-air gravity and topography. Examination of the geology as well as topography reveals the effect of topography completely masks the geology. For example, the dense (2.76) metamorphosed limestones of the North Tumacacori Foothills do not create a closed anomaly as is present in the geology and Bouguer anomaly maps. Subsurface density distributions are usually the sources of anomalies of interest. Therefore, the local free-air anomalies can be considered "noise", or in the strictest sense of the definition, "regional" anomalies, since they obscure anomalies of interest to this study (Aiken, in preparation).

Sumner, Schmidt, and Aiken (1976) have shown a correlation between isostasy and the intersection of the zero free-air contour with higher density bedrock. They state (1976, p. 7) that "Southeastern Arizona appears to be in isostatic equilibrium, and the free-air anomaly

zero contour closely outlines the pediment edge of higher density bedrock." The southwestern part of the state seems to reflect the nearby presence of the East Pacific Rise as the -10 to -20 mgal contour more closely fits the pediment edge. The transition to negative contours begins at approximately  $110^{\circ}30'W$  longitude (Sumner et al., 1976, p. 8).

Examination of the geologic and free-air maps shows a correlation of the -25 mgal contour to the pediment boundary and -15 mgal contour to the bedrock surface. This finding does not agree with the data of Sumner et al. (1976), and may be due to the increased resolution of a 1:62,500 scale versus the 1:1,000,000 scale used in the state map. One possible explanation is that southern Arizona is not as close to isostatic equilibrium as was originally reported.

#### Complete Bouguer Anomaly Map

The Bouguer anomaly is more useful in local gravity analysis because local topographic effects have been minimized. A general correlation with geology can be observed on this map (Figure 5, in pocket). Several features of this map will be discussed for the purpose of comparison with residual maps. First, notice the closed gravity high over the dense limestones of the North Tumacacori Foothills. It is the least negative value on the map. The granitic rocks of Mount Benedict present a closed high 14 mgal lower than the limestones. This is a reflection of the regional gravity; Bouguer anomaly values steadily decrease to the southeast. The trend of the contours east of Mount Benedict and Nogales does not seem to follow geology or structure. Examination of regional and residual anomalies will reveal the reason.

The Santa Cruz Valley seems to be divided into several sections. The northernmost opens toward Tucson and is part of a larger structure in the Green Valley area (Davis, 1967). Four other closed lows dominate the basin gravity.

#### Regional-residual Calculation and Separation

Identification and removal of regional gravity anomalies may be accomplished through any one of several methods (Dobrin, 1960; Nettleton, 1976). In this study a double Fourier series computer program developed by Carlos Aiken will be used to generate regional trend surfaces. Formulation of the algorithm by James (1966) is discussed in detail by Robinson (1975) and Goodoff (1975).

Generation of regional anomalies using a double Fourier series is both quick and repeatable. The important fact is that the surface generated must be justified. The surface removed must eliminate unwanted trends and isolate the anomaly of interest.

#### Regional Elevation Datum

Aiken (1976, p. 73) has shown a positive correlation between the long-wavelength Bouguer anomalies and trends of station elevations. This positive correlation is a direct consequence of the removal of the gravitational effect of the mass of isostatically compensated topography by a reduction datum defined by mean sea level or at least a horizontal surface (Aiken, in preparation). Basic theories of isostasy require this correlation because the higher the crust extends above sea level

the thicker the crust is below sea level and the more negative the Bouguer anomaly (due to the crust being lighter than the mantle).

Digitized terrain correction data ( $3^{\circ} \times 3^{\circ}$  blocks) were used to generate a double Fourier trend surface of elevations with a fundamental wavelength of 1200 miles (1920 km). The surface generated constitutes an intermediate datum between sea level and station elevation. This trend surface and the deGraaf-Hunter equation (Aiken, 1976, p. 37)

$$g_{GH} = g_{FAT} - 2\pi G\rho(h - h_m) \quad (10)$$

where  $g_{FAT}$  = terrain corrected free-air anomaly in milligals

$\rho$  = density (2.67 g/cc)

$h$  = station elevation in feet

$h_m$  = elevation in feet of the topographic trend surface

are used to calculate the first order residual Bouguer gravity values (regional elevation datum). Figure 6 is the regional surface calculated for the thesis area. The First Order Residual Bouguer Gravity Anomaly Map: Regional Elevation Datum (Figure 7, in pocket) is equal to complete Bouguer anomaly minus the regional surface seen in Figure 6.

#### First Order Residual Bouguer Anomaly Map

Initial examination of this map reveals that while the shape of the anomalies is very similar, the values are all much less negative than on the Complete Bouguer Anomaly Map (Figure 5). The gravity highs over the North Tumacacori Foothills and Mount Benedict area just north of Nogales are now of similar magnitude (-20 mgal) and not 14 mgal different,

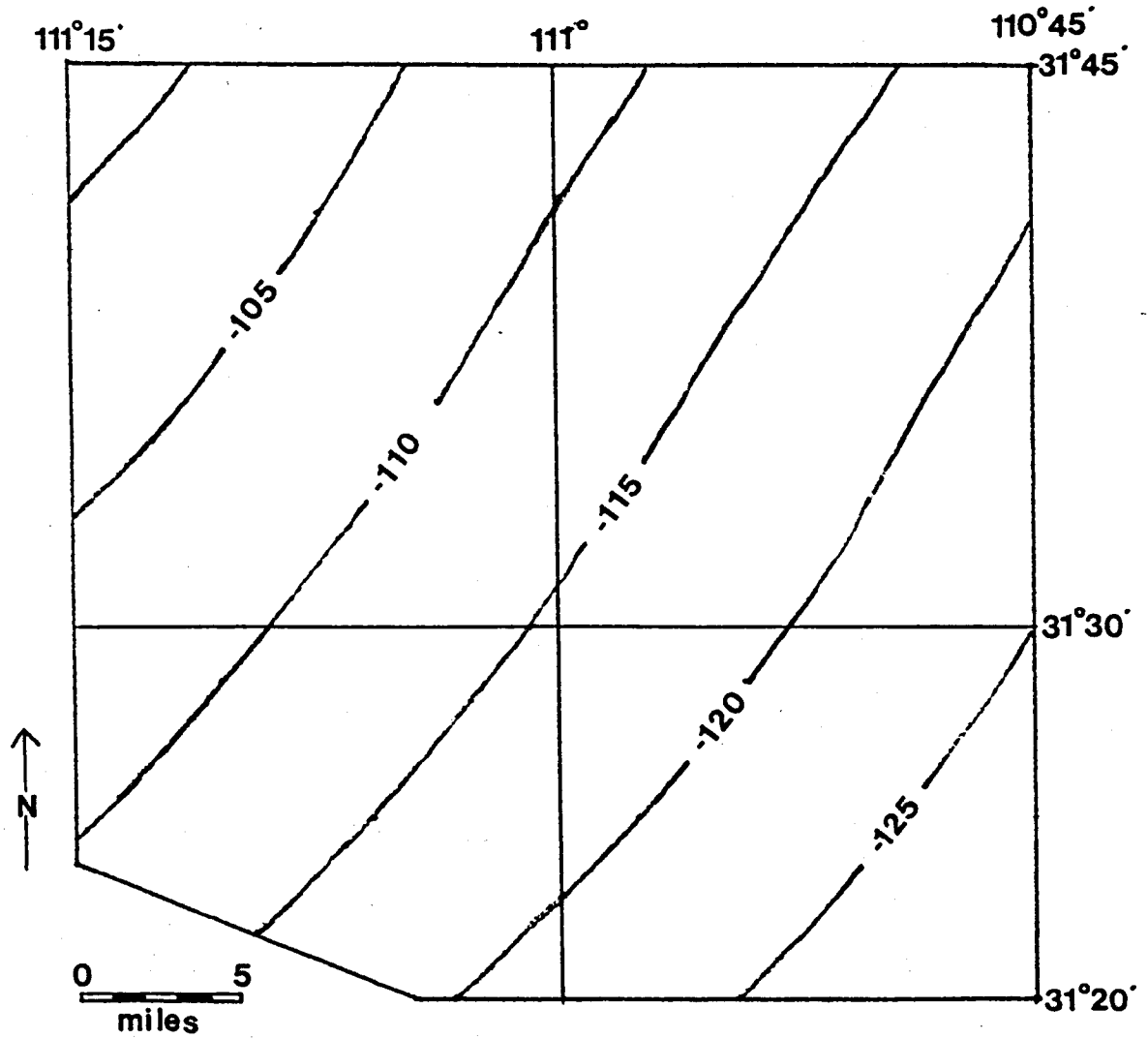


Figure 6. First Order Regional Anomaly Map: Regional Elevation Datum. -- Contour interval = 5 mgal.

as they were in Figure 5. The same effect is noted in the basin, where three major lows of nearly equal magnitude now dominate the structure. The southernmost closed low (west of Nogales) has now become a secondary feature in magnitude.

Perhaps the most striking difference between this map and Figure 5 is in the secondary study area east of Nogales. A definite closed high occurs over sediment, and contours are associated with it to the north parallel to the Patagonia Mountains. These contours are more related to geology than those of Figure 5 because the masking effect of the regional has been removed.

Some very definite trends of contours appear on this map. These are interpreted as faults and are all seen to be extensions of surface features.

A closed gravity low exists in the Ruby area. It is part of the downdropped block west of the Atascosa Mountains. The western fault boundary of the Atascosa Mountains is very pronounced on this map and the gravity low does not directly correlate with alluvium. Most of the anomaly is due to low density silicic volcanics and a displacement on the fault of several thousand feet. The alluvium covers Tertiary volcanics and is not a typical Basin and Range valley.

#### Bedrock Surface

Residual values ideally should be zero on bedrock several miles from the alluvium-bedrock contact. All regional anomalies would then be removed and only the gravity anomaly of the alluvial fill basin would be seen.

Near-surface regional anomalies produced by bedrock may be calculated using the same double Fourier series program. Over 600 terrain corrected bedrock stations from the surrounding area were used to generate the surface. Fundamental wavelengths of 80 miles (north-south) by 35 miles (east-west) were used. Aiken (1976) recommends a fundamental wavelength at least 2.3 times the area of interest. The bedrock regional surface (Figure 8) is nearly planar and varies by only 1.7 mgal over the entire study area.

#### Second Order Residual Map

Removal of the bedrock surface from the first order residual leaves the second order residual Bouguer anomaly (Figure 9, in pocket). Values now are zero over dense bedrock and near zero over much of the mountainous areas. There is almost no difference in the contours of the two residual maps with the exception of value. This map will be used for modeling and interpretation. Location of contours has been checked several times to minimize interpolation errors (see "Errors in Interpretation").

#### Two Dimensional Modeling

Determination of basement structure and depth was accomplished through the use of a two dimensional iterative Fortran computer program written by West (1971). The theory for the program was developed by Bott (1960) and refined by Morris and Sultzbach (1967). Program ITMOD calculates the gravitational attraction of a two dimensional rectangular prism given by



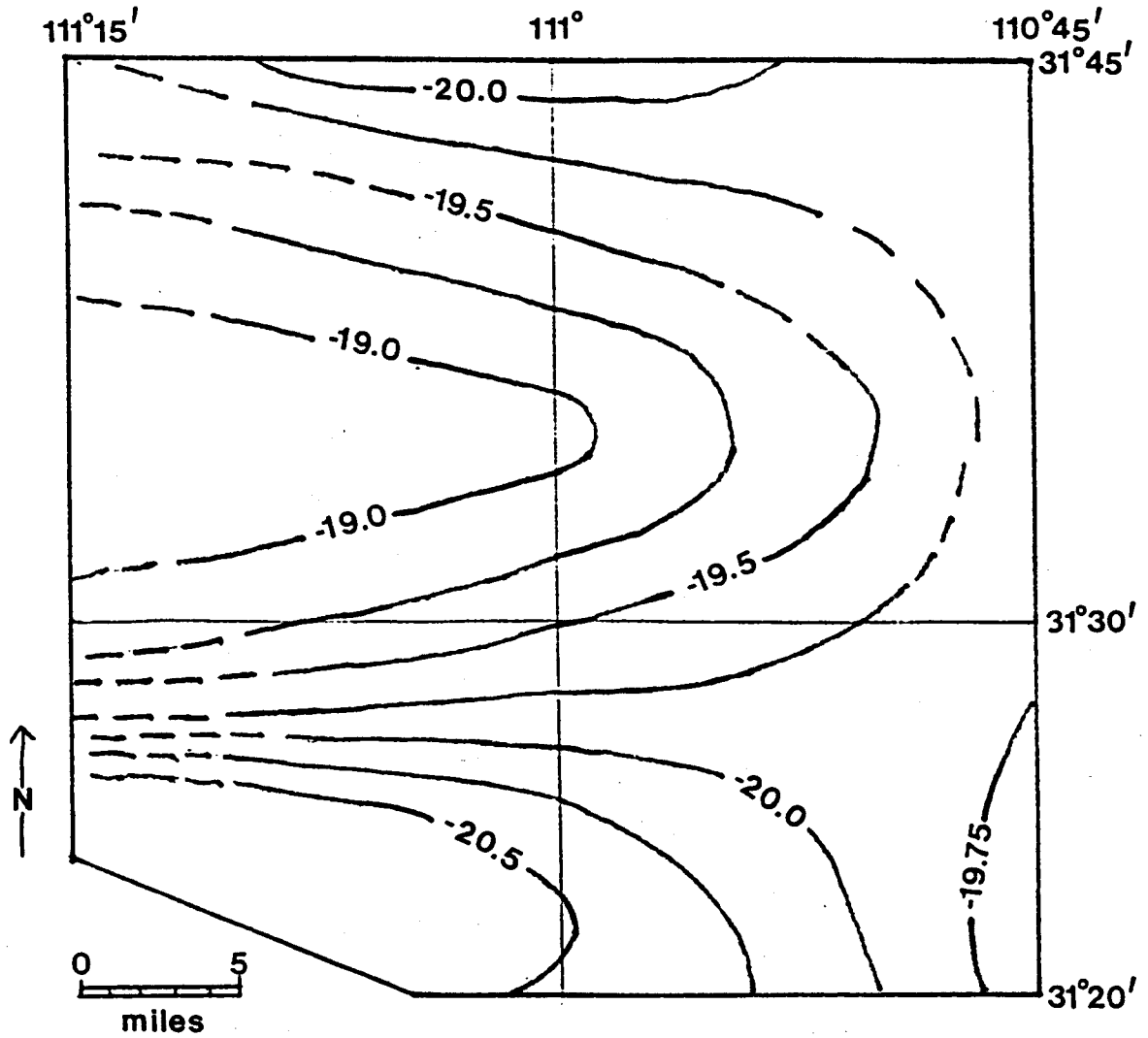


Figure 8. Regional Bedrock Surface Map. -- Contour interval = 0.25 mgal.

$$\begin{aligned}
g = 2G \Delta\rho & X_1 \ln \left( \frac{Z_2^2 + X_1^2}{Z_1^2 + X_1^2} \right)^{\frac{1}{2}} - X_2 \ln \left( \frac{Z_2^2 + X_2^2}{Z_1^2 + X_2^2} \right)^{\frac{1}{2}} \\
& + Z_2 \tan^{-1} (X_1/Z_2) - \tan^{-1} (X_2/Z_2) \\
& - Z_1 \tan^{-1} (X_1/Z_1) - \tan^{-1} (X_2/Z_1)
\end{aligned} \tag{11}$$

where  $G$  = universal gravity constant

$\Delta\rho$  = density contrast

$X_1, X_2$  = horizontal distances of the observer from the sides of the rectangle

$Z_1, Z_2$  = the vertical distances of the observer from top and bottom of the rectangle, respectively.

A residual gravity curve is calculated from eq. (11) and compared to the actual residual curve. The difference between the two is used to calculate a new thickness using the Bouguer slab relationship

$$D = D_o + g_r / 2\pi G \Delta\rho \tag{12}$$

where  $D$  = new thickness

$D_o$  = old thickness

$g_r$  = residual gravity difference

$G$  = universal gravitational constant

$\Delta\rho$  = density contrast

Iterations continue until a specified limit is reached.

Results of the iteration are unique for each model and the geologic input parameters. A valley with up to four different density layers

may be modeled with this program. A simple one layer model is used in this study for all profiles due to the absence of any density data from drill hole samples.

#### Density Contrast

Selection of the density contrast is the most problematical of the geologic input parameters. Bedrock contacts may be inferred directly from surface geology, but alluvium density may vary from 1.5 g/cc to 2.5 g/cc (Telford et al., 1976, p. 25). Density also increases with depth and age of alluvium; the shallower the basin the greater the contrast.

Much of the alluvium in the Upper Santa Cruz Valley is dissected and therefore recent alluvial deposits are limited. In some areas the valley is only 6 miles wide. Extreme basin depths (over 7000 ft) are therefore considered unlikely. Bedrock densities have been shown to be in the vicinity of 2.65 g/cc and the assumed average alluvial fill density of 2.25 g/cc leads to a contrast of -0.4 g/cc for modeling purposes. This is in agreement with the conclusions of Davis (1967) from acoustic and neutron logs. Several authors (West, 1970a; Aiken and Sumner, 1974; Bittson, 1976; Hargan, 1978) have bracketed models around an average of -0.4 gm/cc contrast. While this value of -0.4 gm/cc is debatable, it is believed to be the best for this valley on the basis of all available data.

### Profile Analysis

Six profiles were drawn across the valley (see Figure 9, in pocket, for locations) perpendicular to gravity contours wherever possible. Profiles may not be accurate in those areas where the two dimensional assumption does not apply. Figures 10 to 15 are models very similar to the computer profiles. Each model is calculated assuming the valley surface is planar and zero depth is equivalent to the surface. The residual anomaly presented in these figures is the observed residual against which the calculated residual for each model in the lower half of each figure is compared. The only places where the observed residual differs by more than 0.5 mgal from the calculated residual is at the bedrock-alluvium contact. Here the author has removed the inconsistencies and smoothed the profile. Hence, the models shown are interpretations of the plotted output of program ITMOD.

All of the following references to subsurface faults are interpretations of the author. These structures are actually buried scarps. Howell (1957, p. 256) defines a scarp as "an escarpment, cliff or steep slope of some extent along the margin of a plateau, mesa, terrace, or bench." The author believes the cause of these buried scarps to be Basin and Range faulting. Gravity modeling is not sensitive enough to distinguish between a large scarp and a zone of small scarps. Hence, all scarps may be scarp zones and faults may be fault systems.

Line A-A' (Figure 10) crosses the large gravity low north of the San Cayetano Mountains from west to east. No pediment is present on the east side, but a 6° buried pediment surface on the west leads to a fault

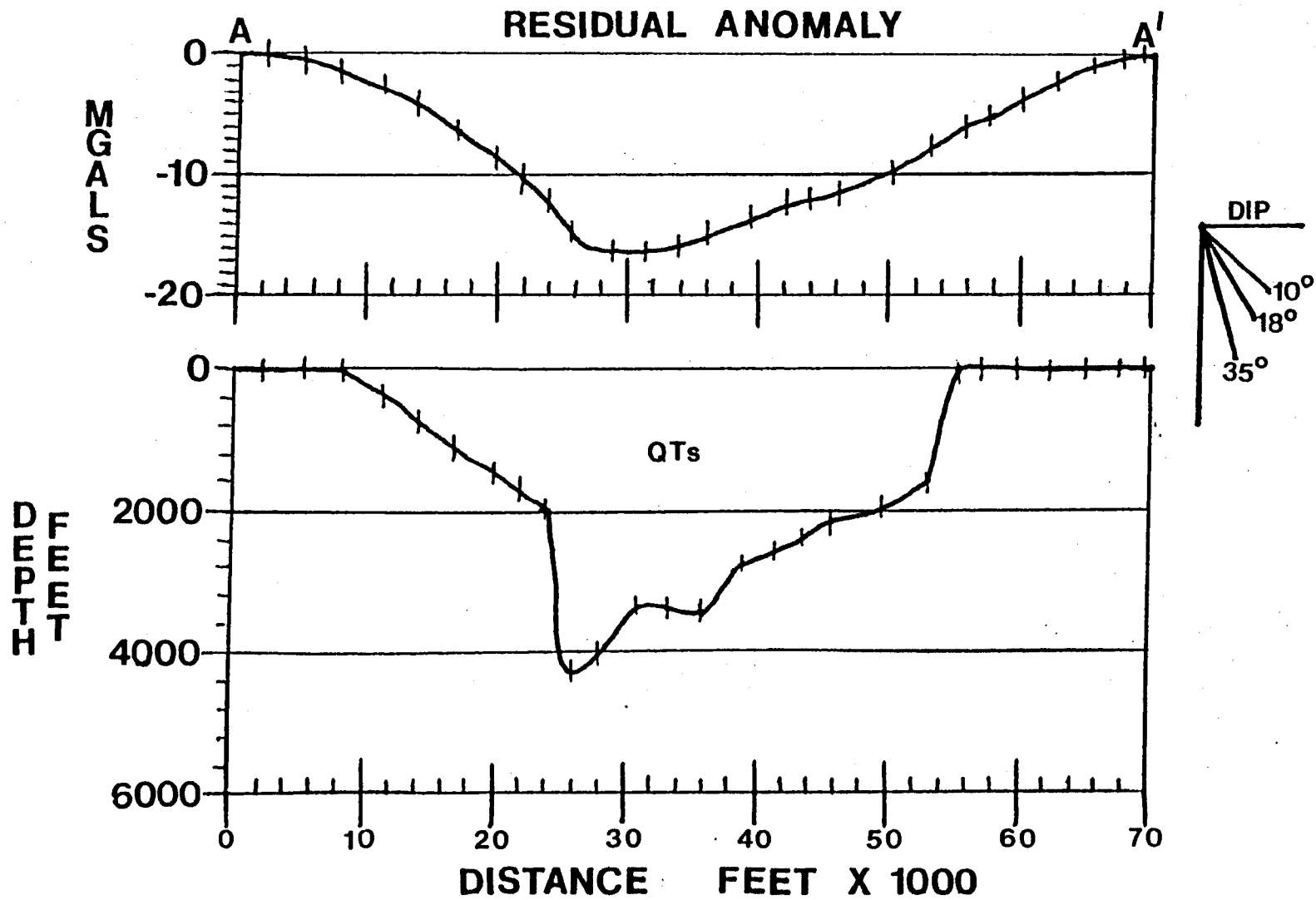


Figure 10. Profile A-A'. -- Vertical exaggeration = 5.40.

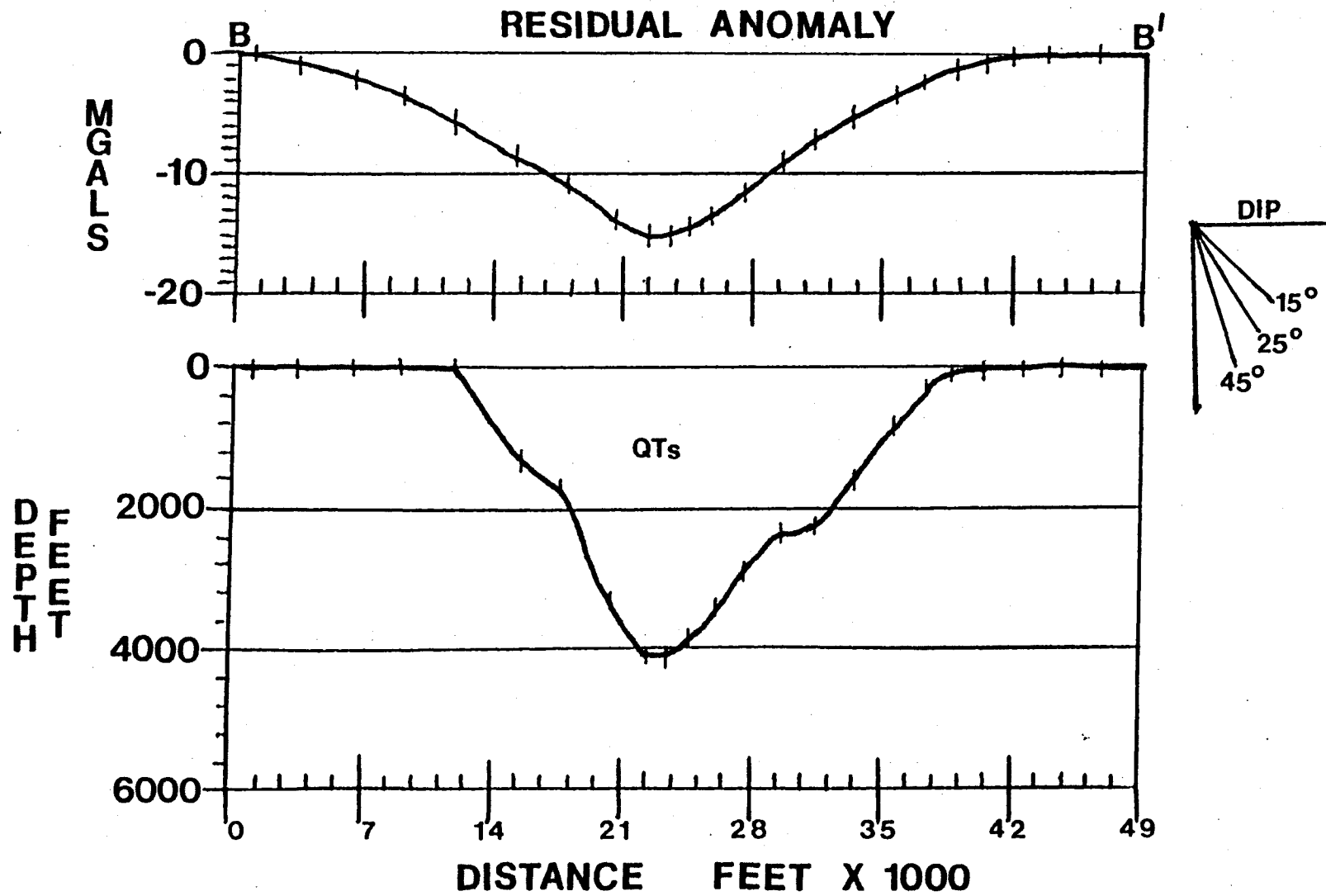


Figure 11. Profile B-B'. -- Vertical exaggeration = 3.75.

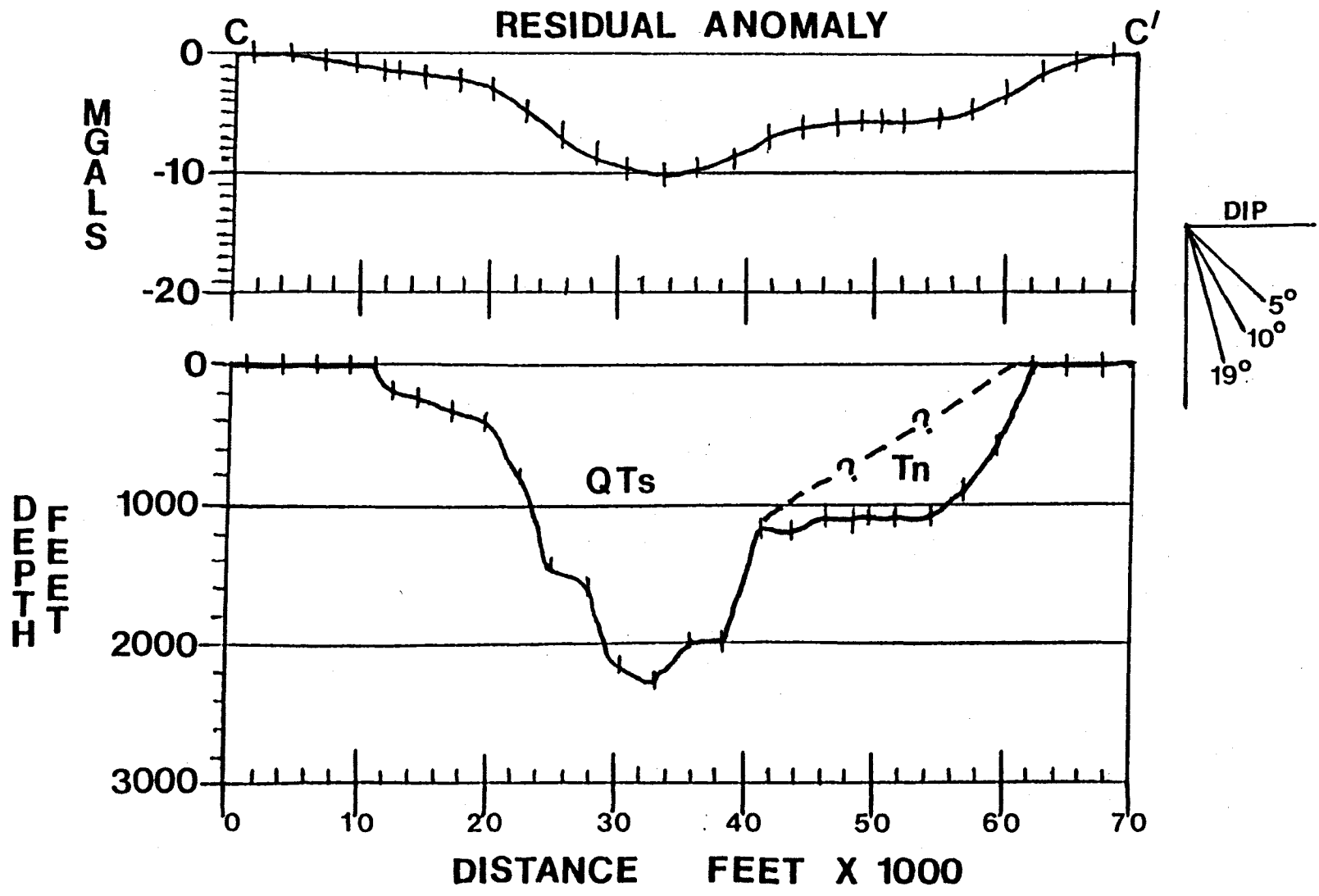


Figure 12. Profile C-C'. -- Vertical exaggeration = 10.75.

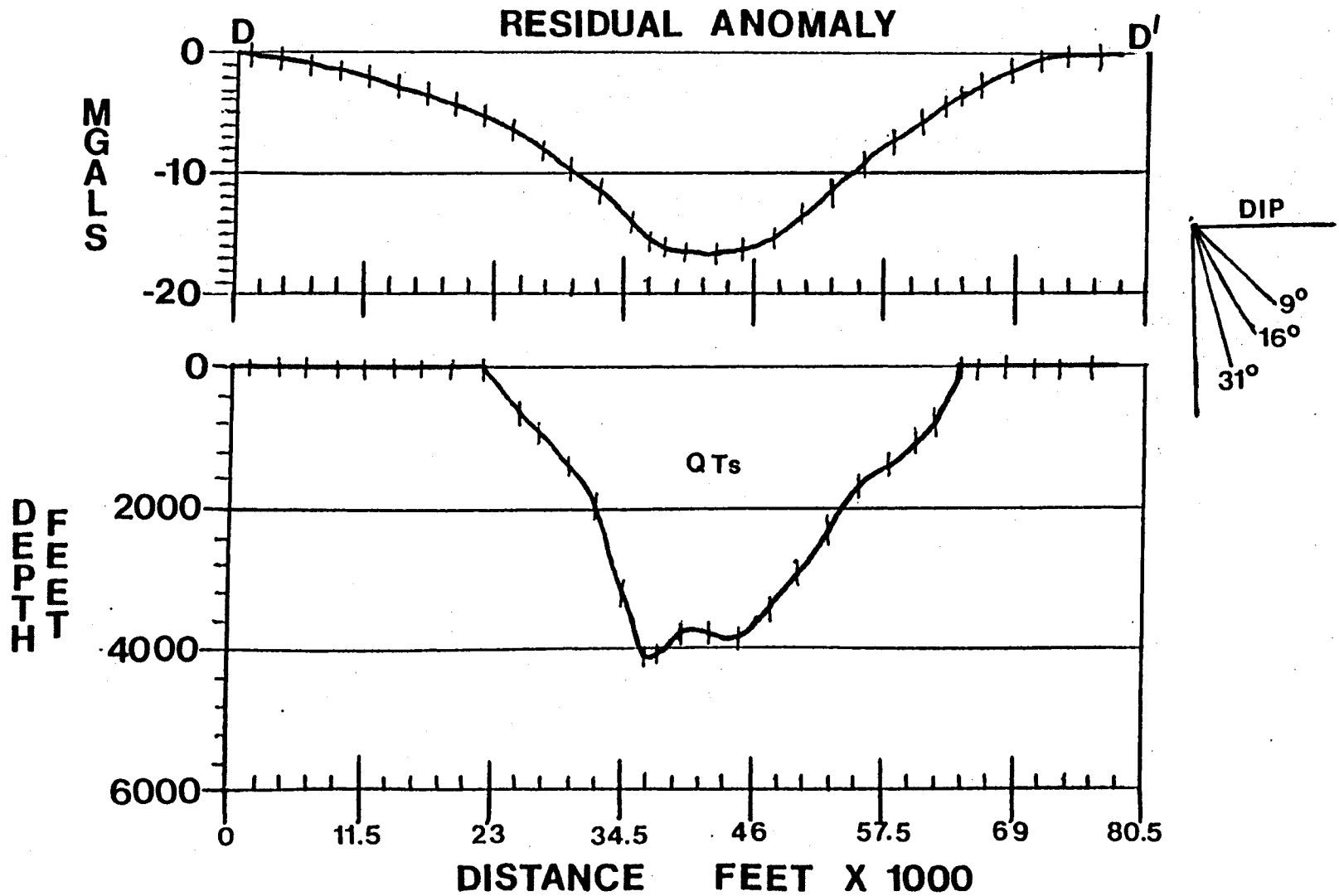


Figure 13. Profile D-D'. -- Vertical exaggeration = 6.15.



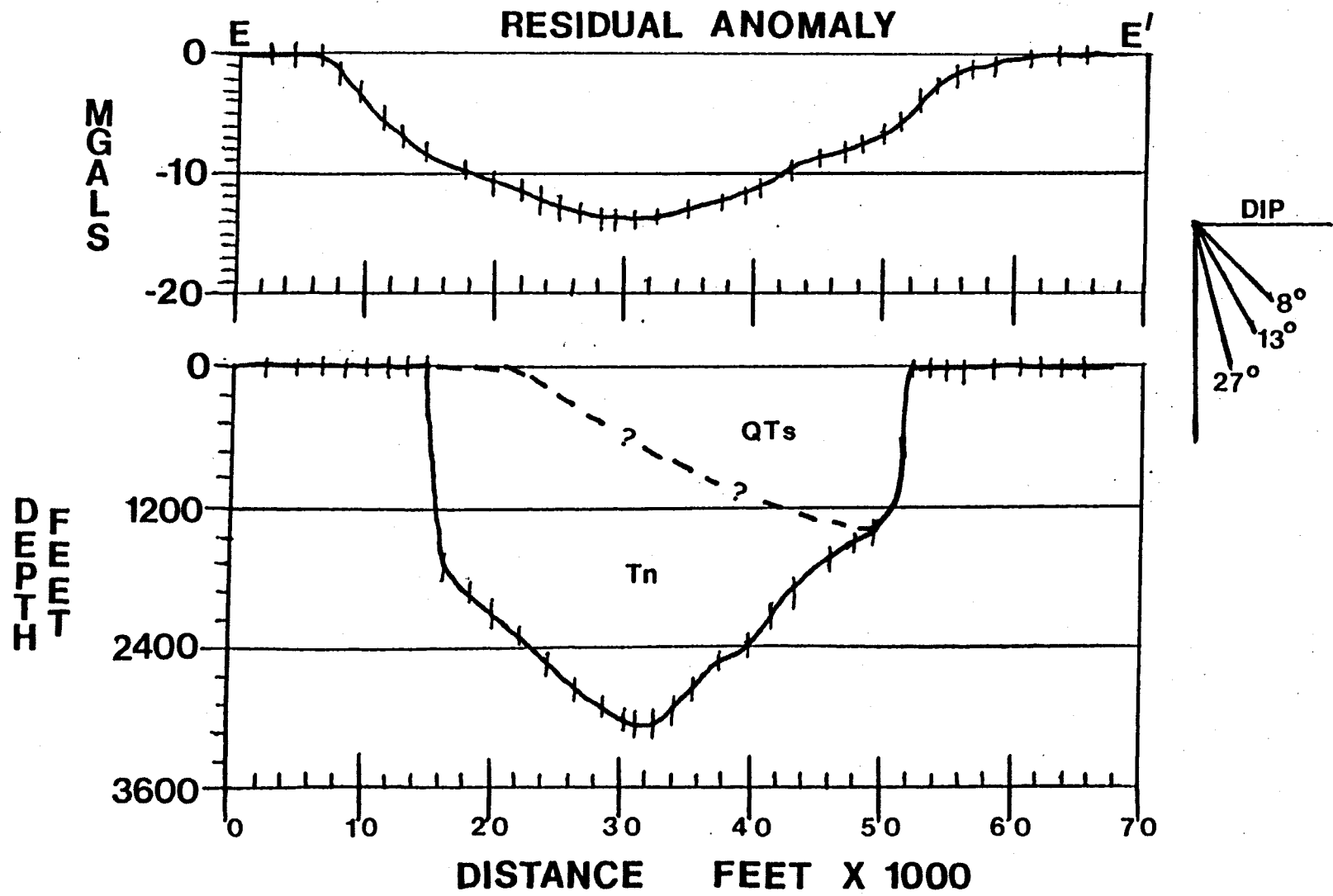


Figure 14. Profile E-E'. -- Vertical exaggeration = 7.45.

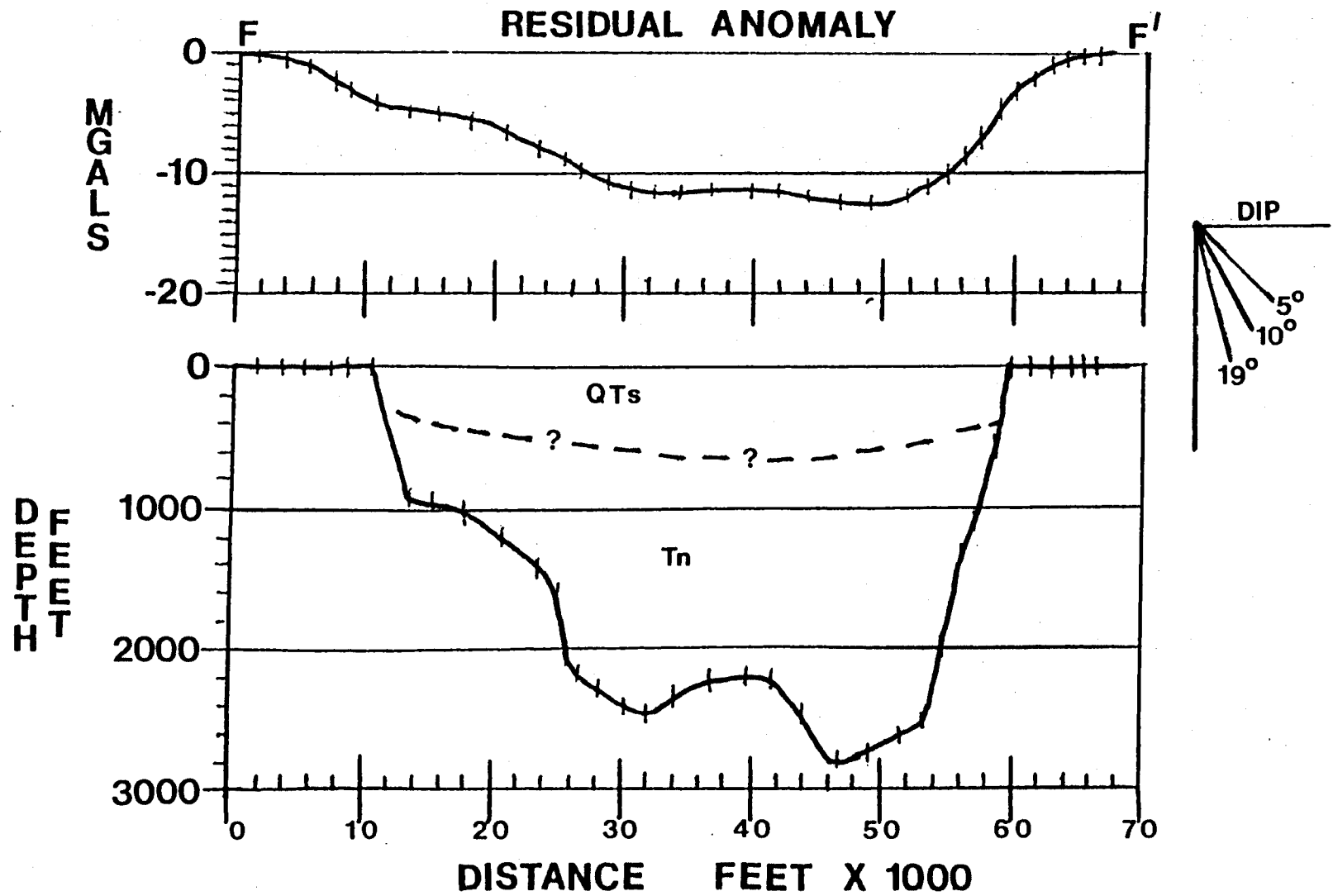


Figure 15. Profile F-F'. -- Vertical exaggeration = 10.75.

with 2000 ft of displacement. The east side scarp has about 1700 ft of displacement and could possibly be an extension of the San Cayetano fault mapped by Drewes (1972). The general structure is that of a graben 4100 ft deep, with the west side being downdropped 2000 ft farther than the east.

Profile B-B' (Figure 11) crosses a gravity low from the Atascosa Mountains east to the San Cayetano Mountains. No real pediment is seen on either side, and two high-angle step faults bound the west basin. Two lower angle faults or possibly a granitic intrusive form the east boundary. The basin reaches 4000 ft in depth in the west-central portion of the valley.

Line C-C' (Figure 12) crosses a high point in the basin floor four miles north of Profile A-A'. Profile C-C' showed the best agreement between actual and calculated residual gravity, but interpretation is complicated by the presence of Nogales Formation and the numerous faults of Drewes' (1972) Montosa Canyon structural block.

The western side has a 2 mile buried pediment which slopes  $3^{\circ}$  to a fault system with about 2000 ft of displacement. One mile to the east of the maximum depth to bedrock of 2400 ft is a scarp which forms the other side of the interpreted graben structure. Nogales Formation (Tn) outcrops under alluvium near the east bedrock contact and forms a pediment-like surface down to the fault plane. The formation could be in the bottom of the valley as well, but is not included due to the increase in density with depth. (Compaction is assumed to make the Nogales Formation nearly equal to bedrock in density.)

Profile D-D' (Figure 13) crosses Profile A-A' and ends in the San Cayetano Mountains. Data at the northwest (D) end of the line are not two dimensional, but agreement with Line A-A' is excellent after the major north-south fault west of the Tumacacori Mountains is crossed. Figure 13 presents the profile after the northwest end is adjusted to agree with Profiles A-A' and C-C'. This cross-section of the valley is an asymmetric graben, the southeast side of which slopes at about  $13^{\circ}$ .

Profile E-E' (Figure 14) extends from the Atascosa Mountains north-northeast to the Sonoita Creek area. The west end crosses the surface expression of a major fault which the previous four profiles show extends northward along the Tumacacori Mountains. This system shall be referred to as the Santa Cruz Fault System. East of the Santa Cruz Fault System is an outcrop of rocks very similar to the Nogales Formation. Nearly 2000 ft of displacement are indicated by the gravity, but that value is possibly much greater due to the presence of faulted Tertiary rocks (Tn?). The fault on the east side shows about 1800 ft of displacement.

It is the interpretation of the author that Nogales Formation underlies much of the valley south of Sonoita Creek. Profile F-F' (Figure 15) is assumed to be underlain by Nogales Formation along its trace from the Pajarito Mountains to Mount Benedict. A major fault has uplifted the Mount Benedict block (in agreement with Simons, 1974) and the Santa Cruz Fault System forms the western half of the graben structure.

Depth to Bedrock  
and Basin Structure Map

The results of two dimensional modeling and the Second Order Residual Bouguer Anomaly Map (Figure 9) have been used to create the Subsurface Basin Configuration: Interpretation Map (Figure 16, in pocket). This map is almost wholly interpretative; it is the final result of analyzing all geologic and geophysical data.

Scarps drawn on this map are well-documented by profiles, the Second Order Residual Bouguer Anomaly Map, and geologic mapping. They are all extensions of or parallel to visible or implied surface faults.

The depth to bedrock contours are highly interpretative and are very influenced by unknown geology; i.e., Nogales Formation. The Nogales Formation probably underlies all of the southern third of the valley, as well as the area just southeast of Mt. Hopkins in the Santa Rita Mountains. The general shape of the basin is still very similar to that of the gravity maps. Depths may be inaccurate due to lack of well control and subsurface basin density measurements.

Ground Water Available from Storage

While the interpretation of gravity anomalies is inherently ambiguous in terms of mass distributions, there is a method for determining the magnitude of the mass causing the anomaly (Hammer, 1945). This method involves the use of Gauss' mathematic theorem as adapted to gravity and measured over the upper planar surface of a hemisphere (Ramsey, 1940). West (1970a) discusses the topic extensively. The

relationship used to calculate the anomalous mass of the basin is (Grant and West, 1965, p. 227-228)

$$2\pi G \Delta M = \int_{-\infty}^{\infty} \int_{-\infty}^{\infty} g(x,y) dx dy \quad (13)$$

where  $\Delta M$  is the anomalous mass. The integration was evaluated by summing the contributions of each square mile of the anomaly area in gals. A residual map with all nonvalley-fill gravitational effects removed (all bedrock away from the valley is zero) was created from the results of ITMOD profiles. Where the zero contour was out of the study area, the limits of the thesis area were chosen as boundaries. For the Upper Santa Cruz Valley

$$\Delta M = \frac{-2.0147 (2.59 \times 10^{10})}{4.191 \times 10^{-7}}$$

$$\Delta M = -1.2451 \times 10^{14} \text{ kg.}$$

The area of the primary basin is 218 square miles.

The total volume of saturated alluvium in the basin is calculated by removing the volume of alluvium above the water table. West (1970a) gives this formula as

$$V_1 = \frac{\Delta M - \Delta \rho_2 h S}{\Delta \rho_1} \quad (14)$$

where  $\Delta M$  = anomalous mass from eq. (13)

$V_1$  = volume of saturated sediments

$h$  = depth to water table

$S$  = surface area of basin

$\Delta \rho_1$  = contrast in density of wet sediments and bedrock

$\Delta \rho_2$  = density contrast between dry alluvium and bedrock.

Values chosen for  $\Delta\rho_1$  and  $\Delta\rho_2$  are  $-0.4$  g/cc and  $-0.7$  g/cc, respectively and are in agreement with those of West (1970a). Bradbeer (1978) calculates  $h$  as 40 ft in the Sonoita Creek-Rio Rico golf course area; this is in agreement with values given the author by residents of the study area and will be used as the average for the entire basin. The results of these calculations are presented in Table 3 along with those in Avra Valley and Tucson Basin for comparison.

Table 3. Volume of Saturated Alluvium.

Location	$m$ ( $10^{14}$ Kg)	$h$ (feet)	$S$ ( $\text{mile}^2$ )	$V_1$ (million acre feet)		
				$\Delta\rho_1 =$ $-0.3$ g/cc	$\Delta\rho_1 =$ $-0.4$ g/cc	$\Delta\rho_1 =$ $-0.5$ g/cc
Avra Valley	-2.78	300	510	520	389	274
Tucson Basin	-5.35	200	850	1190	892	717
Upper Santa Cruz Valley	-1.245	40	218	323	243	194

To compute the volume of ground water available,  $V_1$  is multiplied by the percentage of water in the saturated alluvium, or storage coefficient. West (1970a) uses a coefficient of 0.15 calculated from pumping and run-off data. Davis (1967) calculates 0.05 for the Tucson Basin storage coefficient from downhole density logs. Bradbeer (1978)

uses 0.30 for recent alluvium at the confluence of Sonoita Creek and the Santa Cruz River. She also makes the assumption in her thesis that seepage through Nogales Formation at Lake Patagonia is negligible. This implies a very low storage coefficient for this formation.

Because of the differences in storage coefficients, values will be calculated at 0.15, 0.10, 0.05, and presented with data from Avra Valley and Tucson Basin for comparison (Table 4). Because West's (1970a) value was for near-surface alluvium and the presence of Nogales Formation in much of the basin, 0.10 will be used here as the most probable value.

Approximately 24 million acre feet of water are available in the Upper Santa Cruz Valley. It must be emphasized that this calculation does not include water quality or technical or economic feasibility of removal.

#### Errors in Interpretation

The largest source of error in a study such as this is in interpretation. Errors in data accumulation are constant, but errors of interpretation are sporadic and hidden to most readers. As more data become available, it is usually wise to reinterpret an area, beginning by recontouring the complete Bouguer or First Order Residual: Regional Elevation Datum anomalies.

Interpretation errors in contouring are very random. Care must be taken to carefully place each contour between data points and to recognize and remove bad stations. Poor elevation control and high near-station terrain corrections will be obvious when contouring.



Table 4. Volume of Ground Water Available.

Location	Storage Coefficient	Volume (Million Acre Feet)		
		$\Delta\rho_1 =$ -0.3 g/cc	$\Delta\rho_2 =$ -0.4 g/cc	$\Delta\rho_3 =$ -0.5 g/cc
Avra Valley	.15	78.0	58.4	41.1
West (1970a)	.10	52.0	38.9	27.4
	.05	26.0	19.5	13.7
Tucson Basin	.15	179.0	134.0	108.0
Davis (1967)	.10	119.0	89.2	71.7
	.05	59.5	44.6	35.9
Upper Santa	.15	48.5	36.5	29.1
Cruz Valley	.10	32.3	24.3	19.4
	.05	16.2	12.2	9.7

Improper contour placement was found in this study to be the cause of irregularities in two dimensional modeling results. Hand smoothing is not needed if contours are properly placed and prism values accurately chosen. Another source of error in ITMOD profiles is from tailing errors. Endpoints too close to alluvium will cause the depth of alluvium to be too shallow. Insufficient inner terrain corrections will have the same effect.

The choice of the wavelength of the bedrock surface will influence the second order residual. Poor bedrock station coverage around an area of study will also result in an accurate bedrock surface. Because this study area is bounded to the south by Mexico, no bedrock stations were included south of the area in the calculation of the bedrock surface. The low relief of the bedrock surface (Figure 8) does not change the anomalies in the study area and supports the use of a regional elevation datum as a method of regional removal. Future work in the Upper Santa Cruz Valley may be able to improve the bedrock surface.

West (1970a) has estimated the errors in the anomalous mass determination and concludes errors in complete Bouguer anomaly values are the most important. Taking a maximum error of  $\pm 0.6$  mgal against an average residual value of about  $-8$  mgal gives an error of only  $\pm 8\%$  in the anomalous mass.

Geology and choice of density contrasts will greatly influence results of interpretation, but without sufficient data they cannot be

shown to be in error. Using  $-0.3$  g/cc instead of  $-0.4$  g/cc density contrast increases the alluvium thickness by 1800 ft. Each researcher will probably choose these parameters differently.

#### Correlation with Aeromagnetic Data

A portion of the Residual Aeromagnetic Map of Arizona (Sauck and Sumner, 1970) appears in Figure 17. The survey was flown at 9000 ft above mean sea level and flight lines were about 3 miles (5 km) apart. Consequently, the top of any structure reflected in the aeromagnetic anomalies is probably below mean sea level (Aiken and Sumner, 1974).

The two major features of Figure 17 are closed magnetic highs which are due to the Oligocene Grosvenor Halls volcanics and Mesozoic volcanic pile of the Mt. Wrightson area. Volcanics in the northern Patagonia Mountains also associate with a magnetic high. The volcanic rocks of the Tumacacori and Atascosa Mountains do not have a magnetic anomaly associated with them and are therefore assumed not to be deep seated.

Gravity lows in the valley areas do not correlate with magnetic anomalies. This is in agreement with the findings of Aiken and Sumner (1974) for the Basin and Range Province in general. Any correlation between gravity and aeromagnetic anomalies in Figure 17 is related to outcrops of granitic and volcanic bedrock.

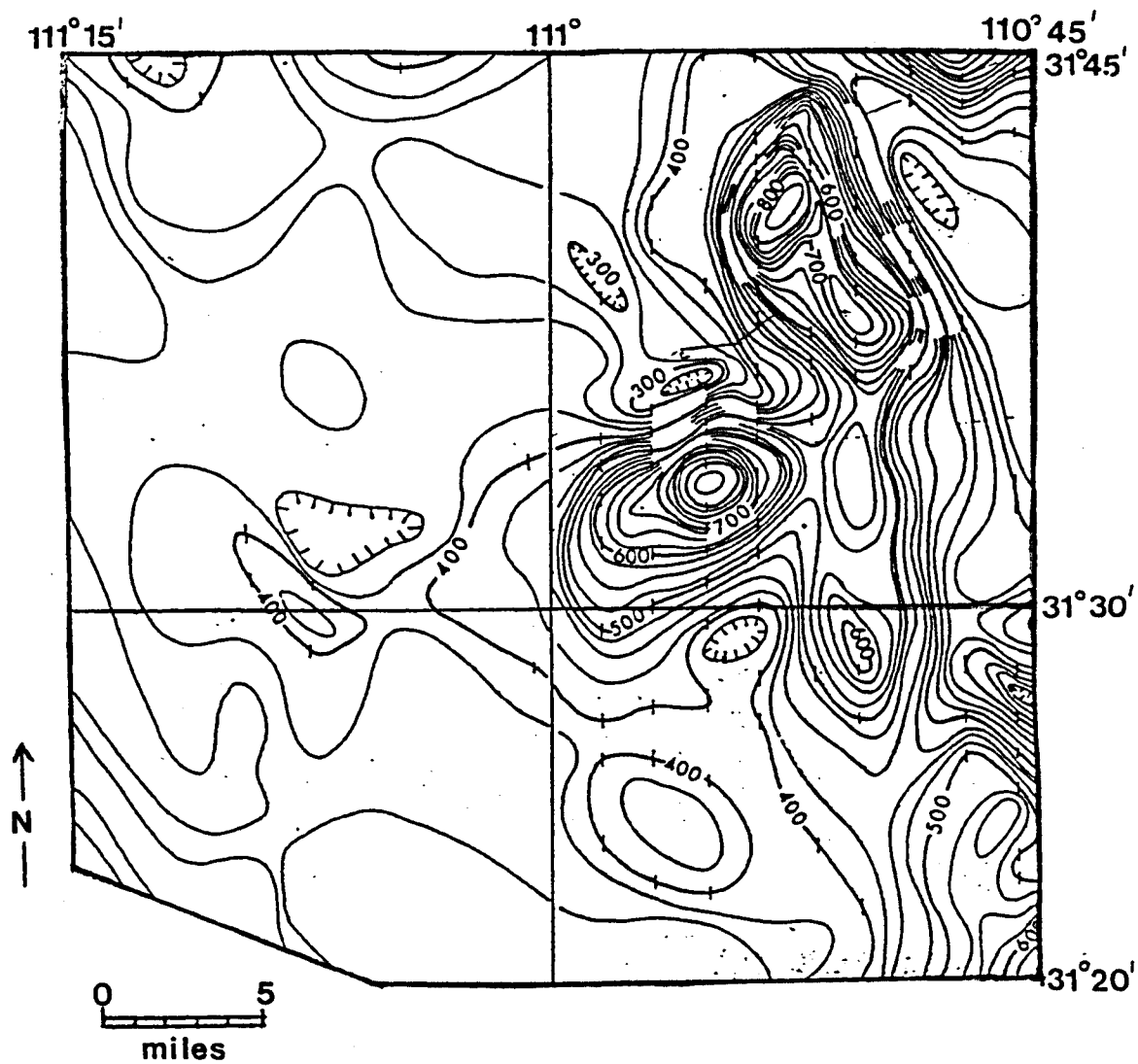


Figure 17. Residual Aeromagnetic Map of the Upper Santa Cruz Valley (from Sauck and Sumner, 1970).

## CONCLUSIONS

The Upper Santa Cruz Valley is a north-south trending graben structure which is closed at the southern end. The primary valley has three depressions, the northmost of which is part of a large basin structure in the Green Valley area. The maximum depth of alluvium in the two closed gravity lows near the San Cayetano Mountains is about 4200 ft. Buried pediments extend about 4 miles into the basin west of Mt. Hopkins in the Santa Rita Mountains and 2 miles east into the basin from the Tumacacori Mountains. The southern third of the valley floor is characterized by gentle slopes and thicknesses of alluvium of no more than 2200 ft. The effect of intermediate density Nogales Formation volcanic detritus and gravels, which probably underlie as much as half the basin within 2000 ft of the surface, will be to lessen the thickness of alluvium and increase depth to bedrock.

The western structural boundary of the valley is formed by a single north-south trending fault system, here known as the Santa Cruz Fault System. The eastern structure of the valley is formed by a complicated array of northwest- northeast-trending scarps. These are interpreted as faults and are all extensions of or parallel to faults mapped on the surface by Drewes (1972) and Simons (1974).

A determination of the anomalous mass of the basin yielded  $\Delta m = -1.25 \times 10^{-14}$  kg with an error of not more than 8%. Using a density contrast of -0.4 g/cc and a storage coefficient of 0.10, a total volume of 24.3 million acre feet of ground water available in storage was

calculated. It is not feasible to remove all of this stored water because of permeability factors.

If large volumes of ground water are pumped from this basin, subsidence may occur (Christie, in preparation). The most probable area for fissuring due to differential compaction would be just east of the Santa Cruz Fault System and subsidence would be greatest between the major scarps in the center of the basin.

Favorable locations for mineral exploration where bedrock is less than 2000 ft below the surface include the pediment areas between the Basin and Range faults and bedrock (Figure 16) and all of the secondary study area east of Nogales. The alluvium-covered area near Ruby is also shallow enough for mineral exploration.

Several drill holes to bedrock in the basin would provide valuable geologic and density data for any future geophysical work.

## REFERENCES

- Aiken, C. L. V., 1975, Residual Bouguer gravity anomaly map of Arizona: Laboratory of Geophysics, Department of Geosciences, The University of Arizona.
- \_\_\_\_\_, 1976, Analysis of the gravity anomalies in Arizona: Unpublished Ph.D. Dissertation, The University of Arizona
- \_\_\_\_\_, in preparation, A Bouguer correction employing a regional topographic datum as a method of computing residual Bouguer gravity anomalies: Department of Geosciences, The University of Arizona.
- Aiken, C. L. V., Schmidt, J. S., and Sumner, J. S., 1975, Free-air gravity anomaly map of Arizona: Arizona Geol. Soc. Digest, 10, Map Suppl., Plate 2.
- Aiken, C. L. V. and Sumner, J. S., 1974, A geophysical and geological investigation of potentially favorable areas for petroleum exploration in southeastern Arizona: Arizona Oil & Gas Conservation Commission, Rept. of Inv. 3.
- Bevington, P. K., 1969, Data Reduction and Error Analysis for Physical Sciences: McGraw-Hill Book Co., New York.
- Bittson, A. G., 1976, Analysis of gravity data from the Cienega Creek area, Pima and Santa Cruz Counties, Arizona: Unpublished M.S. Thesis, The University of Arizona.
- Bott, M. H. P., 1960, The use of rapid digital computing methods for direct gravity interpretation of sedimentary basins: Royal Astron. Soc. Geophys. Jour., vol. 3, no. 1, p. 63-67.
- Bradbeer, G. E., 1978, Hydrogeologic evaluation of the Sonoita Creek aquifer: Unpublished M.S. Thesis, The University of Arizona.
- Christie, F. J., in preparation, Analysis of gravity data from Picacho Basin, Arizona: M.S. Thesis, The University of Arizona.
- Cunningham, J. E., 1964, Geology of the North Tumacacori Foothills, Santa Cruz County, Arizona: Unpublished M.S. Thesis, The University of Arizona.

- Davis, R. W., 1967, A geophysical investigation of hydrologic boundaries in the Tucson Basin, Pima County, Arizona: Unpublished Ph.D. Dissertation, The University of Arizona.
- Dobrin, M. B., 1960, Introduction to Geophysical Prospecting: 2nd ed., McGraw-Hill Book Co., New York.
- Drewes, H., 1971, Geologic map of the Mount Wrightson quadrangle southeast of Tucson, Santa Cruz and Pima Counties, Arizona: U. S. Geol. Survey Misc. Geol. Inv. Map I-614.
- \_\_\_\_\_, 1972, Structural geology of the Santa Rita Mountains, southeast of Tucson, Arizona: U. S. Geol. Survey Prof. Paper 748.
- Garland, G. D., 1970, The Earth's Shape and Gravity: Pergammon Press, New York.
- \_\_\_\_\_, 1976, Introduction to Geophysics: Mantle, Core, and Crust: W. B. Saunders Co., Philadelphia, Pennsylvania.
- Goodoff, L. R., 1975, Analysis of gravity data from the Cortaro Basin area, Pima County, Arizona: Unpublished M.S. Thesis, The University of Arizona.
- Grant, F. S. and West, G. F., 1965, Interpretation Theory in Applied Geophysics: McGraw-Hill Book Co., New York.
- Hammer, S., 1939, Terrain corrections for gravimeter stations: Geophysics, v. 4, p. 184-194.
- \_\_\_\_\_, 1945, Estimating ore masses in gravity prospecting: Geophysics, v. 10, p. 50-62.
- Hargan, B. A., 1978, Regional gravity data analysis of the Papago Indian Reservation, Pima County, Arizona: Unpublished M.S. Thesis, The University of Arizona.
- Hench, S. W., 1968, A reconnaissance gravity survey of the Ruby-Pena Blanca area, Santa Cruz County, Arizona: Unpublished M.S. Thesis, The University of Arizona.
- Howell, J. V., 1957, Glossary of Geology and Related Sciences: American Geologic Institute, Washington, D. C.
- James, W. R., 1966, FORTRAN IV program using double Fourier series for surface fitting of irregularly spaced data: Kansas Geol. Survey Computer Contr. 5, Lawrence, Kansas.
- LaCoste, L. and Romberg, A., 1968, Instruction Manual for LaCoste & Romberg, Inc., Model G Geodetic Grav. Meter, No. 174, Austin, Texas.



- Marsden, L. E., 1960, How the national map accuracy standards were developed: *Surveying and Mapping*, v. 20, p. 427-439.
- Menges, C. M., in preparation, Late Cenozoic evolution of the Sonoita Creek basin; implications for Basin and Range in southeastern Arizona: M.S. Thesis, The University of Arizona.
- Morris, D. B. and Sultzbach, R. A., 1967, Gravity data reduction and interpretation using a digital computer, a case history, in *Mining Geophysics*, Vol. II: Society of Explor. Geophysicists, Tulsa, Oklahoma, p. 630-641.
- Nelson, F. J., 1963, The geology of the Pena Blanca and Walker Canyon areas, Santa Cruz County, Arizona: Unpublished M.S. Thesis, The University of Arizona.
- Nettleton, L. L., 1954, Regionals, residuals, and structures: *Geophysics*, v. 19, p. 1-22.
- \_\_\_\_\_, 1976, *Gravity and Magnetics in Oil Prospecting*: McGraw-Hill Book Co., New York.
- Plouff, D., 1961, Gravity survey near Tucson, Arizona: U. S. Geol. Survey Prof. Paper 424-D, p. 258-259.
- \_\_\_\_\_, 1966, Digital terrain corrections based on geographic coordinates: Paper presented at the 36th Ann. Mtg. of SEG, Houston, Texas, Abstract in *Geophysics*, v. 31, no. 6, p. 1208.
- Ramsey, A. S., 1940, *Theory of Newtonian Attraction*: Cambridge at the University Press, New York, 184 p.
- Robinson, D. J., 1975, Interpretation of gravity anomaly data from the Aravaipa Valley area, Graham and Pinal Counties, Arizona: Unpublished M.S. Thesis, The University of Arizona.
- Sauck, W. A. and Sumner, J. S., 1970, Residual aeromagnetic map of Arizona: Department of Geosciences, The University of Arizona.
- Simons, F. S., 1974, Geologic map and sections of the Nogales and Lochiel quadrangles, Santa Cruz County, Arizona: U. S. Geol. Survey Misc. Geol. Inv. Map I-762.
- Sumner, J. S., Schmidt, J. S., and Aiken, C. L. V., 1976, Free-air anomaly map of Arizona: *Arizona Geol. Soc. Digest* 10, p. 7-12.
- Sumner, J. S. and Schnepfe, R. N., 1966, Underground gravity surveying at Bisbee, Arizona, in *Mining Geophysics*, Case Histories, Vol. I: Society of Explor. Geophysicists, p. 243-252.

- Telford, W. M., Geldart, L. P., Sheriff, R. E., and Keys, D. A., 1976, Applied Geophysics: Cambridge University Press, Cambridge.
- Webb, B. P. and Coryell, K. C., 1954, Preliminary regional mapping in the Ruby quadrangle, Arizona: U. S. Atomic Energy Comm. Tech. Rept., REM-2009, Washington, D.
- West, R. E., 1970a, Analysis of gravity data from the Avra Valley area, Pima County, Arizona: Unpublished M.S. Thesis, The University of Arizona.
- \_\_\_\_\_, 1970b, Geophysical prospecting gravity reduction program: Lab Rept., Laboratory of Geophysics, Department of Geosciences, The University of Arizona.
- \_\_\_\_\_, 1971, Iterative two-dimensional gravity modeling program: Lab Rept., Laboratory of Geophysics, Department of Geosciences, The University of Arizona.
- West, R. E. and Sumner, J. S., 1973, Bouguer gravity anomaly map of Arizona: Department of Geosciences, The University of Arizona.
- Wilson, E. D., Moore, R. T., and Cooper, J. R., 1969, Geologic map of Arizona: Arizona Bureau of Mines and U. S. Geol. Survey.

#75 W.A.  
3065-8

V9791  
1978  
AA7

1997  
A B C  
A B C

1979  
1979  
1979

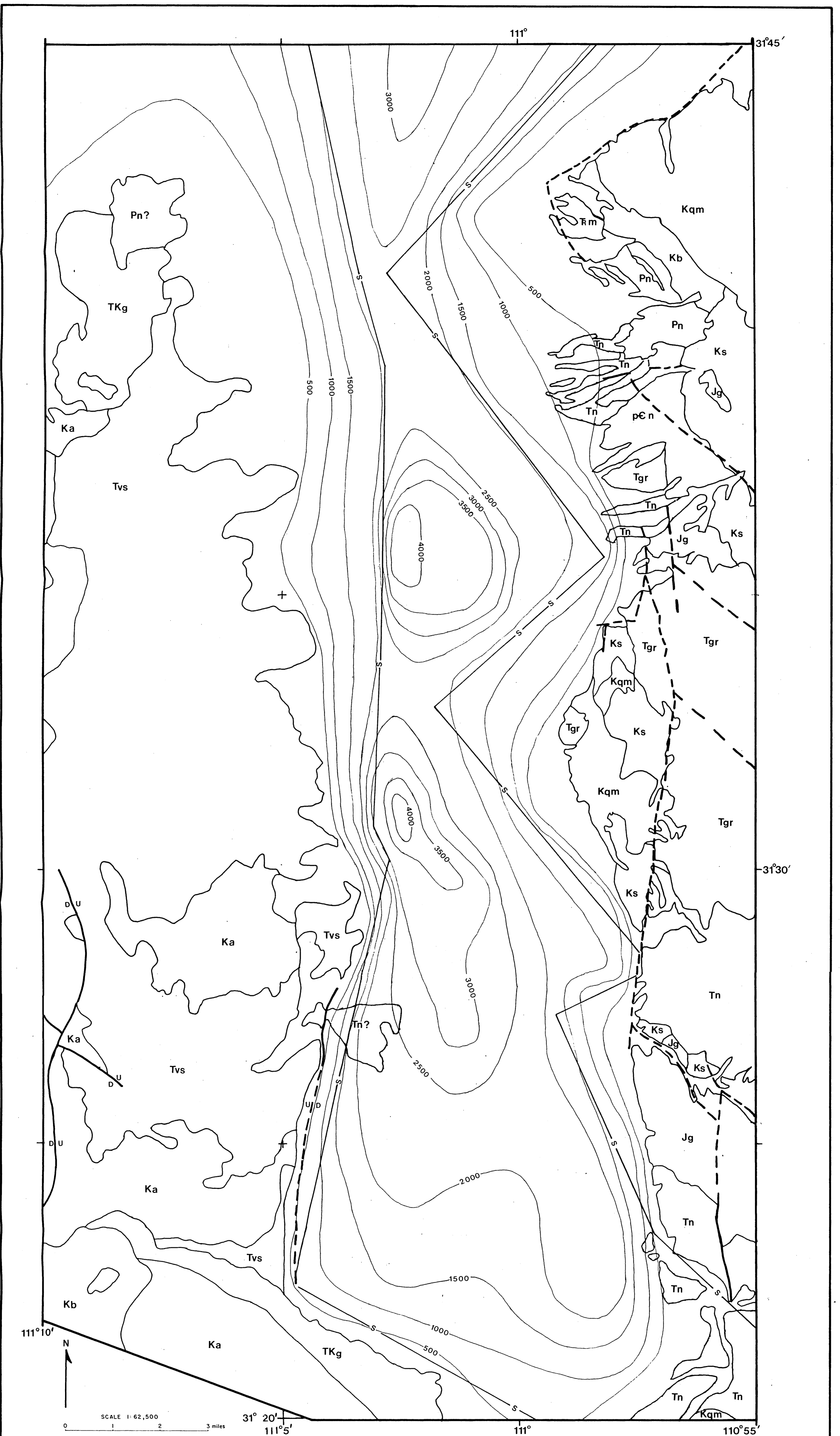
1979  
1978  
447

E9791

1978

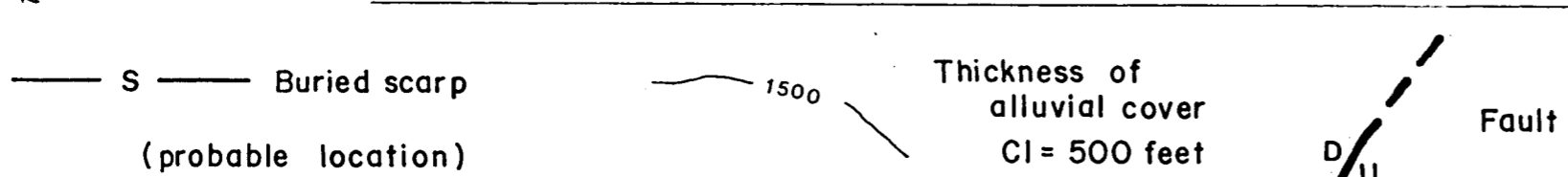
447





**E X P L A N A T I O N**

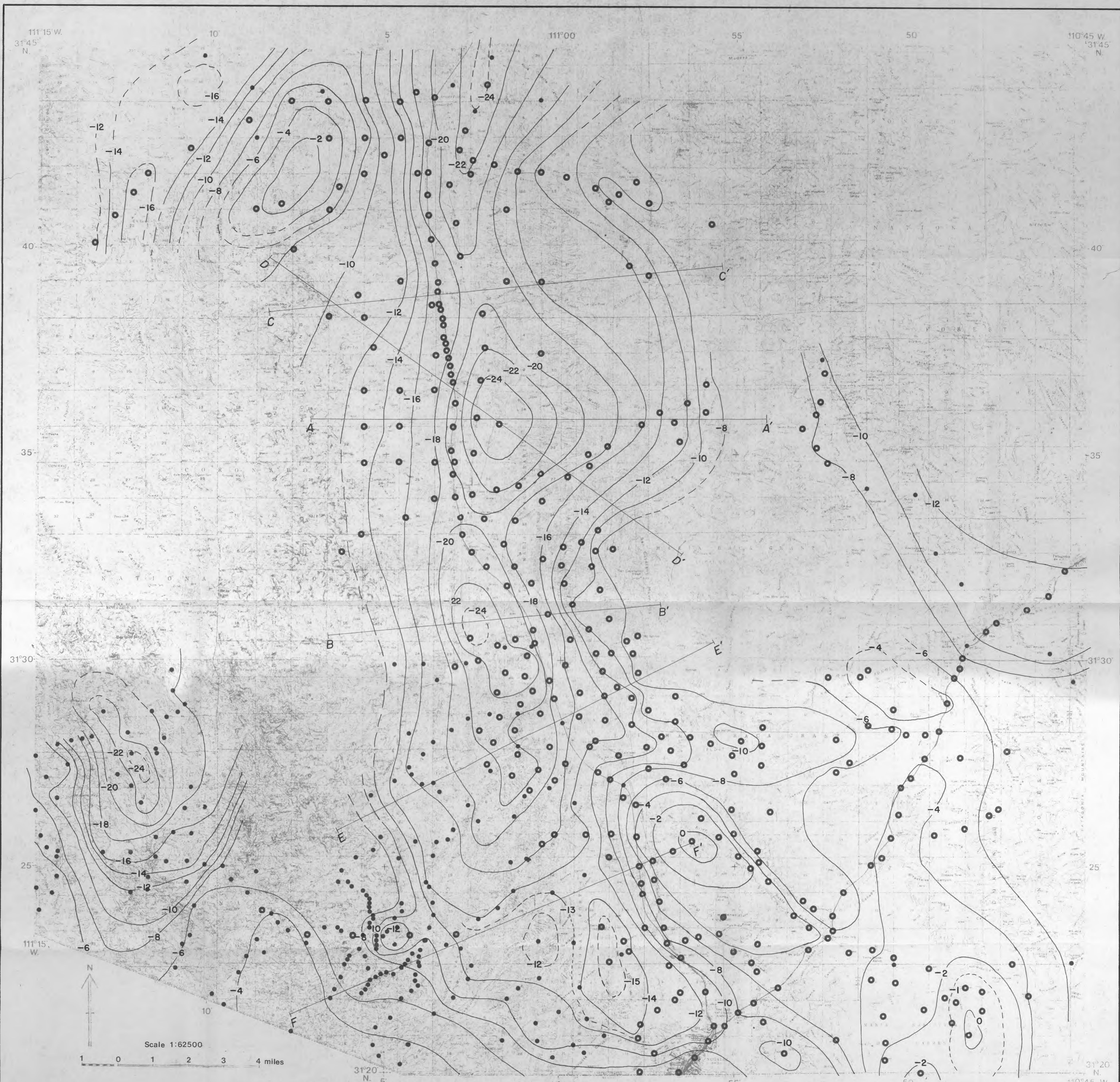
- |  |   |   |
|--|---|---|
| <p><b>QUATERNARY</b></p> <p>QTs— All unconsolidated sediments</p>  | <p><b>TRIASSIC-JURASSIC</b></p> <p>Ks— Undifferentiated tuffaceous sandstone, conglomerate, tuff breccia</p> <p>Kb— Sandstone, siltstone, conglomerate</p> <p>Ka— Andesitic flows and tuffs</p> <p>Kqm— Quartz monzonite and granodiorite</p> <p>Jg— Granite, Mount Benedict quartz monzonite</p> <p>Mzv— Rhyolitic to andesitic flows and pyroclastics</p> | <p><b>PERMIAN-TRIASSIC</b></p> <p>Rm— Mount Wrightson Fm. -- rhyolitic, latitic, andesitic volcanics</p> <p>Rp— Piper Gulch monzonite</p> <p><b>PERMIAN</b></p> <p>Pn— Naco Gp. -- limestones, dolomites, sandstone</p> <p><b>PRECAMBRIAN</b></p> <p>PEh— Hornblende metamorphic and igneous rocks</p> <p>PEn— Gneiss</p> |
| <p><b>TERTIARY</b></p> <p>Tn— Nogales Formation— gravel, conglomerate, sand with volcanic detritus</p> <p>Tg— Biotite hornblende granodiorite</p> <p>Tgr— Grosvenor Hills and Gringo Gulch volcanics -- tuffs</p> <p>Tvi— Intermediate volcanics</p> <p>Tvs— Silicic volcanics</p> | <p><b>CRETACEOUS</b></p> <p>TKg— Granite, quartz monzonite, granodiorite, quartz diorite</p> <p>TKi— Intrusive sills, dikes, plugs</p>  |   |



**SUBSURFACE BASIN CONFIGURATION: INTERPRETATION MAP**

Figure 16

ROBERT W. PARKER  
 M.S. THESIS, 1978  
 UNIVERSITY OF ARIZONA  
 DEPARTMENT OF GEOSCIENCE



# UPPER SANTA CRUZ VALLEY

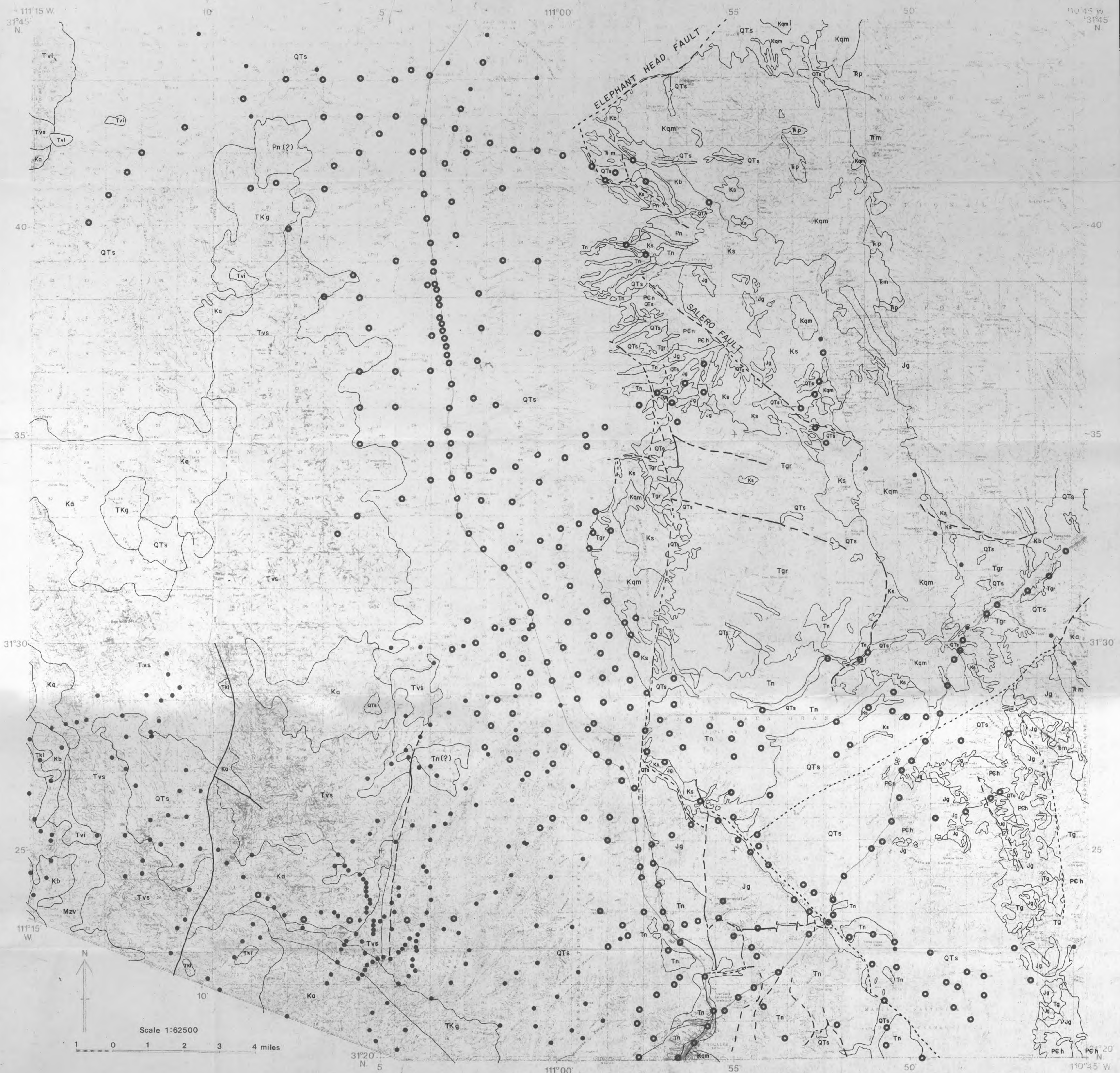
SANTA CRUZ COUNTY, ARIZONA  
1978

SECOND ORDER RESIDUAL  
BOUGUER ANOMALY MAP  
BEDROCK SURFACE REMOVED

- Gravity Station (thesis)
- Gravity Station (Data Base)

Cl = 2mgal

Figure 9

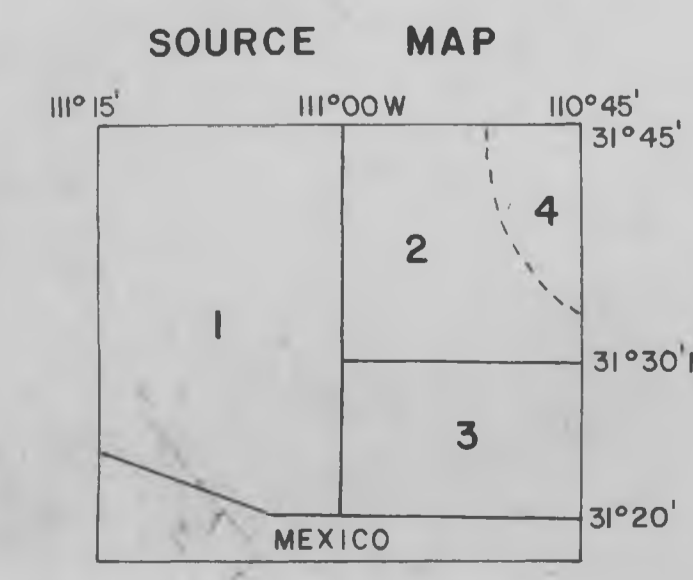


# UPPER SANTA CRUZ VALLEY

SANTA CRUZ COUNTY, ARIZONA  
1978

Figure 3.  
GEOLOGIC MAP

## EXPLANATION



- Wilson, Moore and Cooper, "Geologic Map of Arizona," 1969.
- Drewes, "Geologic Map of the Mount Wrightson Quadrangle," 1971.
- Simons, "Geologic Map and Sections of the Nogales and Lochiel Quadrangles," 1974.
- (not included in study area)

- QUATERNARY**
- QTs - All unconsolidated sediments
  - Tn - Nogales Formation - gravel, conglomerate and sand with abundant volcanic detritus
  - Tg - Biotite hornblende granodiorite
  - Tgr - Grosvenor Hills and Gringo Gulch Volcanics - largely tuffs
  - Tvi - Intermediate volcanic rocks
  - Tvs - Silicic volcanic rocks

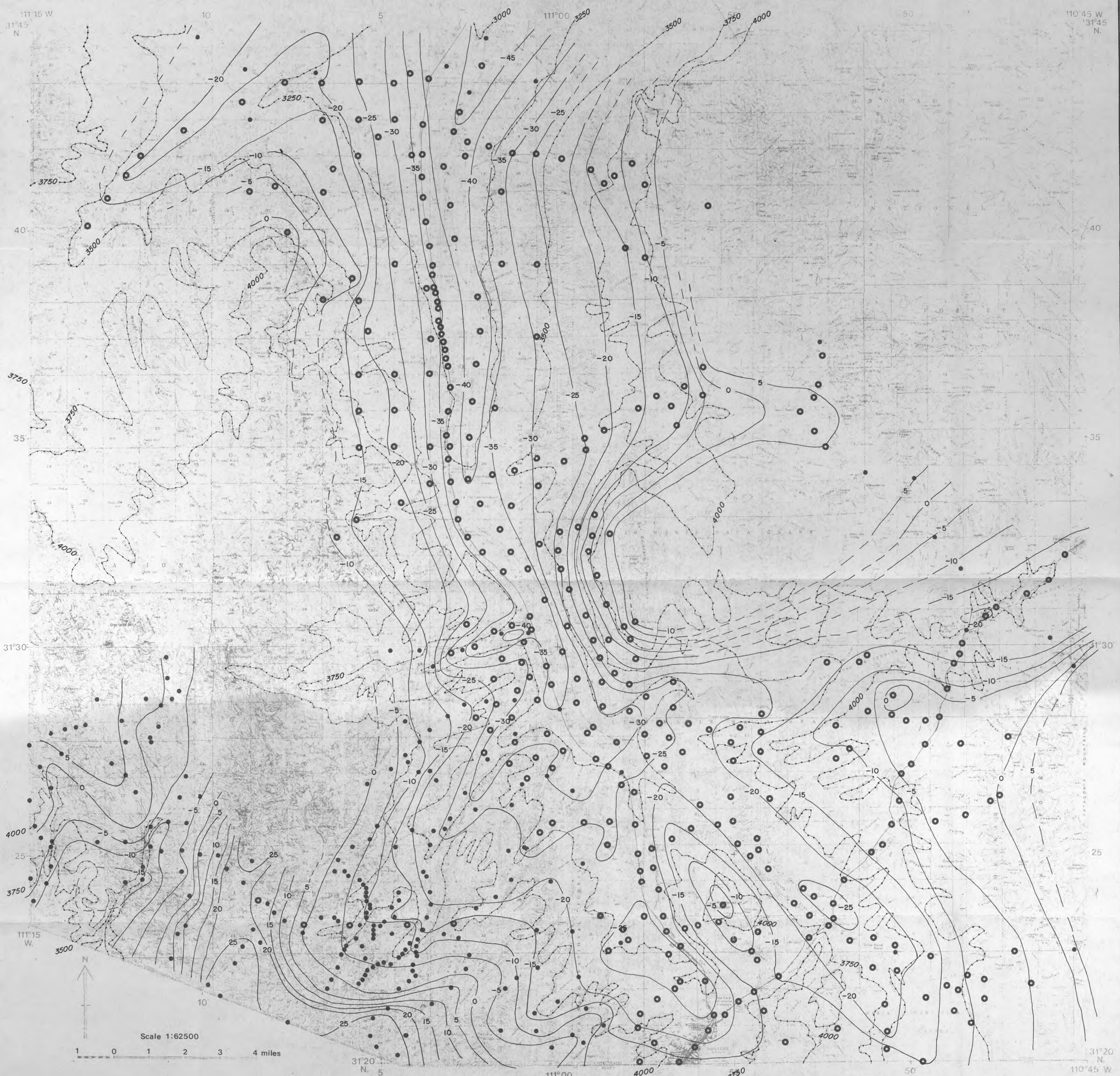
- TERTIARY AND CRETACEOUS**
- TKg - Granite, quartz monzonite, granodiorite and quartz diorite
  - Tki - Intrusive sills, dikes and plugs
  - Ks - Chiefly undifferentiated tuffaceous sandstone, conglomerate and tuff breccia
  - Kb - Sandstone, siltstone, conglomerate
  - Ka - Predominantly andesitic flows and tuffs
  - Kqm - Quartz monzonite and granodiorite

- JURASSIC AND TRIASSIC**
- Jg - Granite and Mt. Benedict quartz monzonite
  - Mzv - Rhyolitic to andesitic flows and pyroclastic rocks
  - Rm - Mt. Wrightson Formation - rhyolitic and latitic volcanics and andesite flows
  - Rp - Piper Gulch monzonite

- PERMIAN**
- Pn - Naco Group - limestone, dolomite and sandstone
  - Pch - Hornblende rich metamorphic and igneous rocks
  - Pcn - Gneiss

- Gravity stations (thesis)
- Gravity stations (Data Base)
- Selected faults

Base map taken from U.S.G.S. 1:62,500 series 1957-58



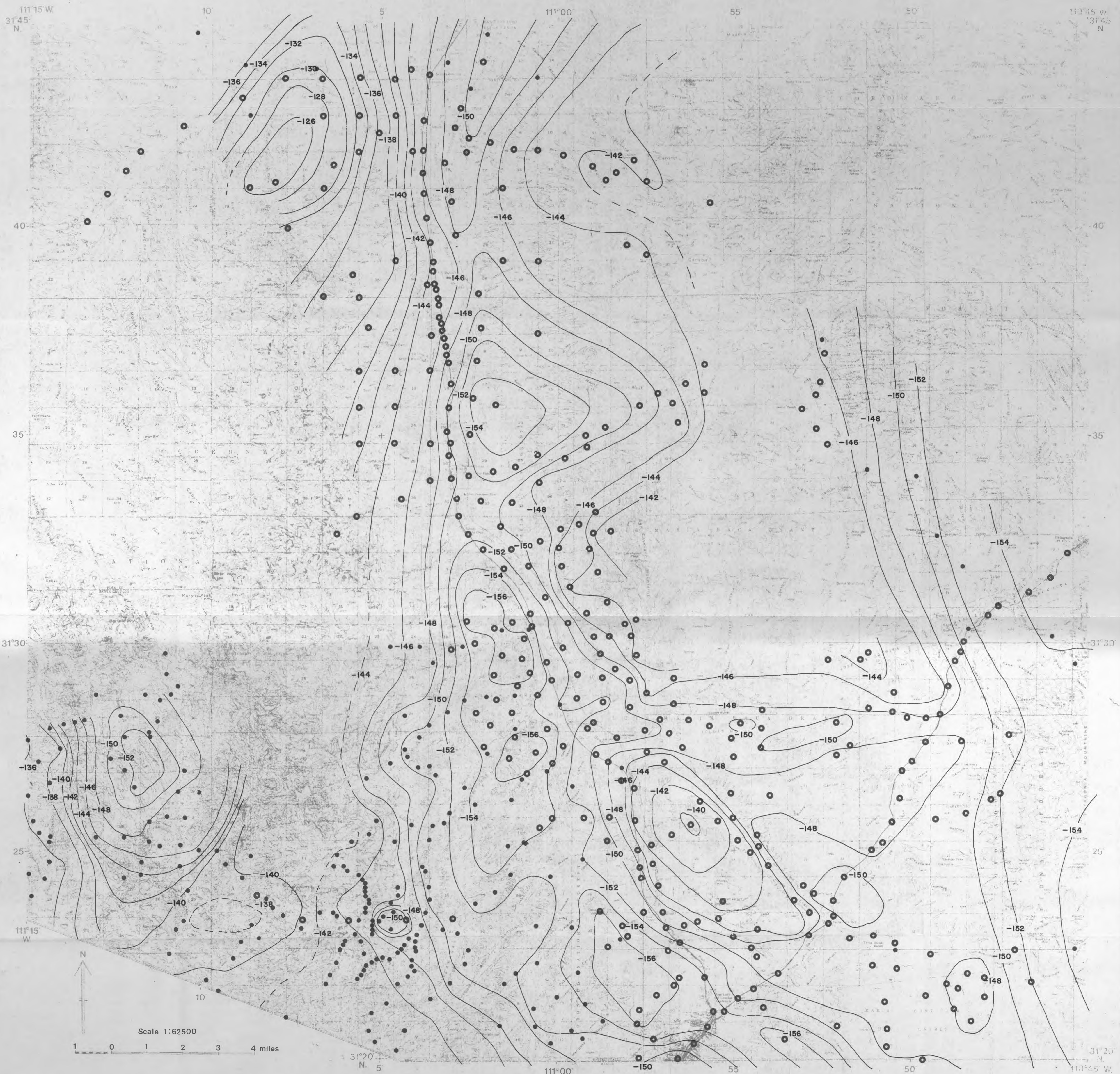
**UPPER SANTA CRUZ VALLEY**  
 SANTA CRUZ COUNTY, ARIZONA  
 1978

**FREE-AIR  
 GRAVITY ANOMALY MAP**

- Gravity Station (thesis)
- Gravity Station (Data Base)
- CI = 5 mgal
- - - CI = 250 feet

**Figure 4**

Base map taken from U.S.G.S. 1:62,500 series, 1957-58



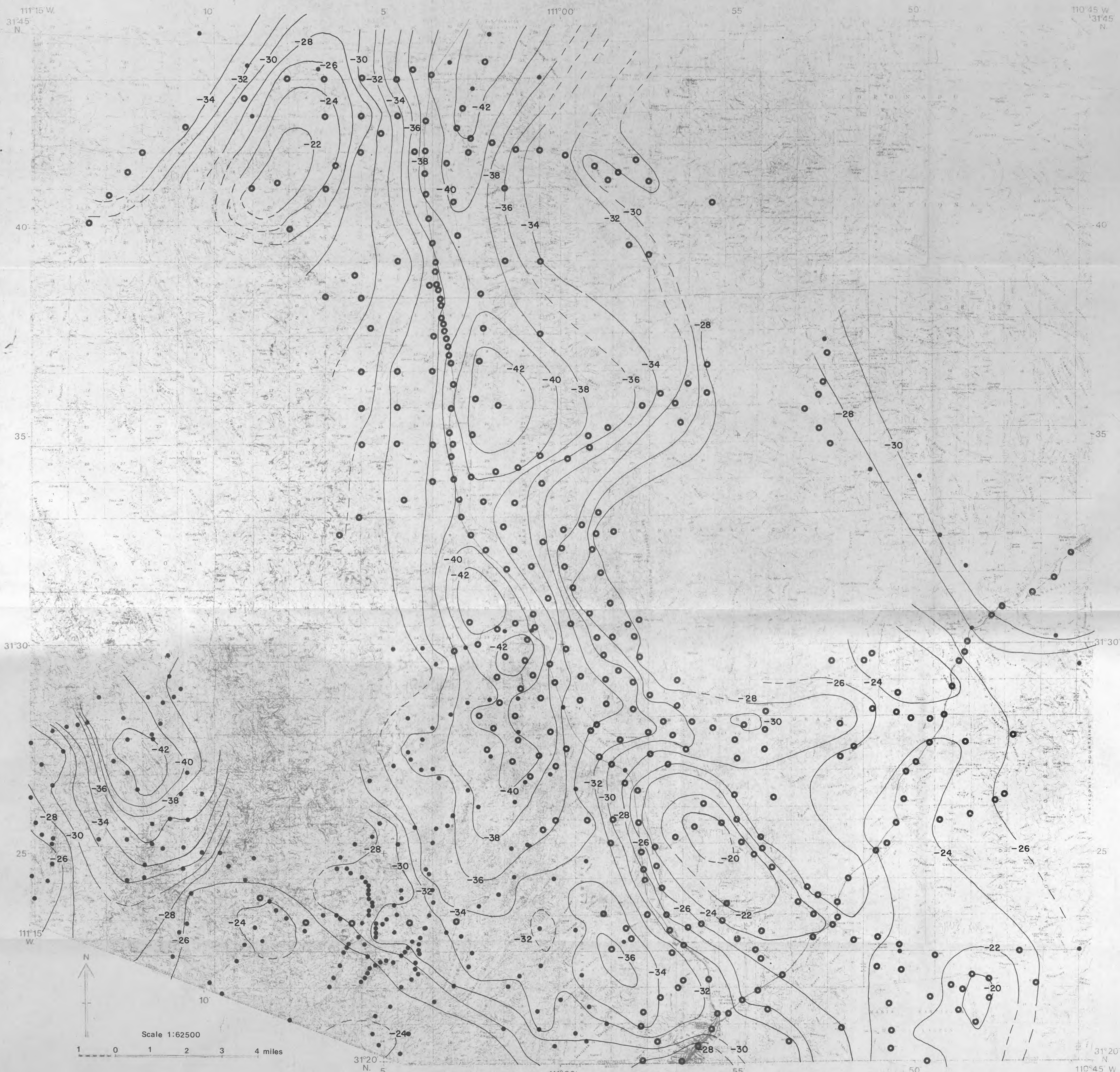
# UPPER SANTA CRUZ VALLEY

SANTA CRUZ COUNTY, ARIZONA  
1978

- Gravity Station (thesis)
- Gravity Station (Data Base)

**COMPLETE  
BOUGUER ANOMALY MAP**

CI = 2mgal  
Figure 5



# UPPER SANTA CRUZ VALLEY

SANTA CRUZ COUNTY, ARIZONA  
1978

FIRST ORDER RESIDUAL  
BOUGUER ANOMALY MAP:  
REGIONAL ELEVATION DATUM

- Gravity Station (thesis)
- Gravity Station (Data Base)

Cl = 2 mgal  
Figure 7